Graph-theoretical Analysis of EEG Functional Connectivity during Balance Perturbation in Traumatic Brain Injury

October 9, 2020

Vikram Shenoy Handiru[1,2], Alaleh Alivar[1] , Armand Hoxha[1], Soha Saleh[1,2] , Easter Selvan[1,2] , Guang Yue[1,2] , Didier Allexandre[1,2] Center for Mobility and Rehabilitation Engineering Research, Kessler Foundation, New Jersey, USA.[2]Department of Physical Medicine and Rehabilitation, Rutgers Biomedical Health Sciences, Newark, USA.

Correspondence should be addressed to Vikram S. Handiru; vshenoy@kesslerfoundation.org

Abstract

Traumatic Brain Injury (TBI) often results in balance impairment, increasing the risk for falls and further injuries. In this study, we investigated the postural instability in a group of 12 TBI patients vs 9 healthy controls (HC) by studying their brain's response to an external perturbation of the computerized dynamic posturography platform. A 64-channel EEG was used to noninvasively record the brain's anticipatory response while the participant was performing the dynamic posturography task. We used the global graph-theoretic network measures (global efficiency and modularity) derived from source-space EEG connectivity in different frequency bands as quantitative measures of the functional integration and segregation of the brain network during the task. The center of pressure (COP) displacement and the Berg Balance Scale (BBS) were used as balance outcomes. Furthermore, we used the Diffusion Tensor Imaging (DTI) data from all the participants to explore the association between the measures of the structural integrity of the white matter (Fractional Anisotropy, Mean Diffusivity, and Mode of Anisotropy) and the balance outcomes.

Our findings revealed significant changes in functional segregation between the TBI group and controls during the task and also group-level differences in DTI measures. Also, we observed significant differences between theta-band modularity and global efficiency during rest vs. task within both the groups (TBI and HC). In terms of the neural correlates, we observed a distinct role played by different frequency bands; increase in theta-band modularity during the task was shown to be highly correlated with the poorer COP displacement and BBS in the TBI group; alpha-band and beta-band graph-theoretic measures were correlated with the measures of structural integrity. In terms of the regions of interest pertaining to the postural control, we noticed a significant cortical activity during the task in the paracentral lobule, post-central gyrus, cingulate gyrus, superior parietal gyrus, and other regions often reported to be involved in postural stability.

Our study, although limited by small sample size, provides insights into the neural correlates of the balance deficits due to brain injury. Our future studies will focus on the larger sample size and also the effect of stabilometry platform training on the functional brain network modulation in TBI.

Introduction

Traumatic Brain Injury (TBI) is a severe medical and health problem in the United States, with an estimated 2.8 million people sustaining a TBI every year (Taylor et al., 2017). TBI patients often suffer from a host of long term cognitive, behavioral, and physical impairments (Sharp et al., 2014). One of the immediate consequences of TBI is an elevated risk of balance deficit or the loss of postural control (Kaufman et al., 2006) (Pickett et al., 2007). Yet, the pathomechanisms of the postural instability remain poorly understood. To develop effective rehabilitation strategies and prognosticating tools for motor recovery, we must delve into the neurophysiological processes involved in postural control.

One aspect that could guide us in this direction is the "functional connectivity" between the brain regions during the postural control task. Functional connectivity refers to the statistical interdependencies between the physiological time series of two regions. In the event of a brain injury, the cortical lesion or the axonal damage can disrupt not only the structural integrity of the white matter but also the functional connectivity between regions (Gratton et al., 2012). Regardless of the type of network (i.e. physical synaptic connection between the set of neurons or the functional connection between two brain regions), a graph theory-based approach is a promising tool to quantify the functional connectivity network organization wherein the whole brain is viewed as a graph with several nodes (e.g. anatomically parcellated region). Using these quantifiable measures to identify the cortical biomarkers of balance deficits in TBI could better guide us in developing intervention strategies. This brings us to three research questions:

(1) *How do the functional networks pertaining to the balance perturbation task change due to TBI?*

(2) *Is the global task-specific* connectivity *measures derived using graph-theory highlight specific brain functional impairment related to balance deficits in TBI?*

(3) *Are task-based functional brain connectivity measures associated with the structural integrity of white matter?*

In pursuit of answers to these questions, we look at the graph-theoretical perspective of brain networks. In this framework, the brain connectivity graph is considered as a network made of nodes and edges. Each node corresponds to a cortical region of interest (based on anatomical/functional parcellation) and the edge corresponds to the strength of the functional connectivity between any two connected nodes. Using these fundamental elements of a graph network, graph theory aims at computing several metrics (i.e. node degree, local and global efficiency, clustering coefficient, modularity, etc.) to characterize and study the functional or structural organization of a network of nodes and edges to better understand the neuroanatomical and neurophysiological basis of brain function. A graphical illustration is presented in Fig. 1 to describe the basic concepts of network neuroscience related to this study.

In particular, the concept of *functional integration* and *functional segregation* is gaining significant attention in the network neuroscience community (Hagmann et al., 2008; Cohen and D'Esposito, 2016; Newman, 2006; Stam, 2014; Rubinov and Sporns, 2010). In this conceptual framework as shown in Fig. 1, the connectivity structure of the brain is considered to be organized in several statistically independent clusters of nodes or subnetworks referred to as *modules.* The nodes in each module are densely connected to each other while being sparsely connected to other nodes of the brain, forming a *community structure (Sporns, 2013).* In this context, the brain must balance its capacity to segregate information within modules to perform a specialized neural function in local circuits, with its ability to integrate information between modules. The functional organization of the brain into modules and their functional integration and segregation are data-driven based on the functional connectivity matrix between all nodes (cortical ROIs in this context). Functional segregation tells us how well the nodes within the modules (cortical ROIs in this context) tend to have a statistical dependence between their time-series (Sporns, 2013). Contrarily, functional integration represents the joint processing of specialized information across subnetworks (or *modules*). For example, we could posit that during balance perturbation brain sub-networks or modules must perform segregated functional tasks such as processing visuo-sensory inputs, planning for the compensatory response, and actually executing the

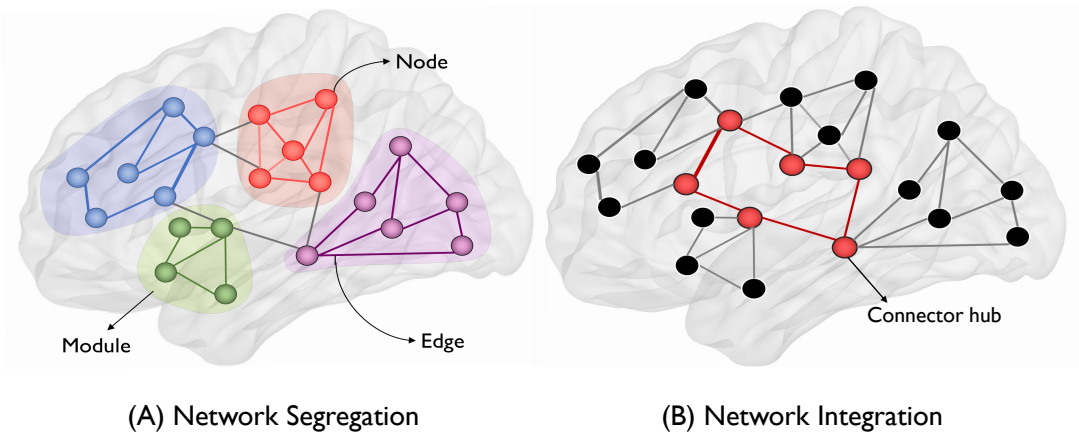

Figure 1: Illustration of graph-theoretic measures. In the context of brain networks in this study, every anatomical region-of-interest is a *node,* whereas the connection between nodes is termed as an *edge.* Colored shaded regions correspond to *modules* which are groups of interconnected nodes but have fewer connections to other modules. On the left, the concept of *network segregation* is illustrated as a network comprising of multiple modules (or segregated sub-networks) whereas, on the right, the *network integration* is illustrated as a group of distant regions interconnected by long-range connections via connector hubs (nodes with a high degree of connectivity).

motor response, while maintaining a certain level of sensorimotor integration between modules to execute a timely, well-measured and coordinated response. For a better understanding of the applications of graph theory in neuroscience, we recommend a review article by (Rubinov and Sporns, 2010).

There is growing evidence that an optimal brain network must have "small-world" characteristics combining strong local connectivity with efficient long-distance connection to achieve a well-balanced functional integration and segregation of neural activity (Rubinov and Sporns, 2010; Stam, 2014). It has been reported that psychiatric and neurological diseases lead to the loss of small-world organization (Lord et al., 2017; Rubinov and Sporns, 2010). Similarly, the structural connectivity network in TBI is shown to deviate from the "small-world" characteristics seen in the healthy brain network (Zhou, 2017). Current literary evidence points to the use of graph-theoretic measures such as node strength (Cao and Slobounov, 2010), local and global efficiency (Caeyenberghs et al., 2014) to study the effect of TBI on postural control.

However, to better understand the dynamic aspects of postural control, one needs to study the association between the posturography/balance control measures and the cortical activity recorded during the motor task. The relevant literature on neuroimaging of postural control in TBI is found in (Diez et al., 2017) wherein the authors reported that in a pediatric TBI population, the postural control indices were correlated with increased connectivity in the prefrontal resting-state functional connectivity. In another study by (Wang et al., 2016), the postural control change and age were shown to have significant interaction with the prefrontal and sensorimotor connectivity, thus indicating the differences in connectivity across age groups. Although these studies demonstrate the correlation between the EEG sensor-based functional connectivity (FC) and postural control (Varghese et al., 2019; Edwards et al., 2018), sensor-space FC must be interpreted with caution because of its spurious nature associated with the inherent challenge caused by volume conduction; instead, the source-space EEG is recommended for measuring the FC (Bastos and Schoffelen, 2015; Shenoy Handiru et al., 2018; Van de Steen et al., 2019).

For a more comprehensive literature on the neuroimaging of human balance control, readers may refer to the systematic meta-analysis review article (Wittenberg et al., 2017). As most of the aforementioned articles

focus only on healthy individuals (young and elderly), the inferences do not offer a complete understanding of balance deficits in the clinical population suffering from brain injury and stroke. In this direction, there are only very few studies such as (Kasahara et al., 2010; Sacco et al., 2011) where the activation (based on fMRI BOLD signal) in the sensorimotor and supplementary motor areas, and functional connectivity patterns within the motor network were shown to be compromised in individuals with TBI.

In a preliminary study published by our group, we showed that the N1 amplitude (a type of event-related negative potential) and the center of pressure (COP) displacement were lower in the TBI group as compared to healthy controls (Allexandre et al., 2019). Further we would like to investigate the changes in cortical connectivity due to balance control in TBI and healthy individuals. We hypothesize that the lower-limb motor deficit in TBI could be associated with the altered functional connectivity during a balance perturbation task.

#Current understanding of postural control studies with EEG recordings#

While several studies investigated the changes in the cortical activity during the lower-limb motor tasks (Wittenberg et al., 2017; Slobounov et al., 2013; Munia et al., 2017), the current understanding is still inadequate. Not only should we be able to quantify the functional measures using kinematic factors (e.g., trajectory, center of pressure, limits of stability, etc.) but also be able to complement the underlying neurophysiological mechanism of balance control through multimodal information. Thus, in this article, we present a group-level analysis of structural and functional mechanisms of postural instability in TBI patients.

#Introduce the functional connectivity studies#

Notwithstanding the published literature on functional connectivity changes during postural control tasks in healthy individuals (Varghese et al., 2019; Wang et al., 2016), the studies are scarce in the clinical population. This motivated us to bridge the knowledge gap of the neural correlates of balance deficits in TBI.

#Reasons for the loss of postural control: DAI after TBI#

The current understanding points to the fact that TBI can cause both focal injuries and diffuse axonal injury (DAI) which disconnects large-scale brain networks (Ham and Sharp, 2012; Sharp et al., 2014). DAI is commonly induced by a sudden acceleration-deceleration or rotational force which is mainly affecting white matter regions such as corpus callosum and subcortical white matter (WM) structures (Adams et al., 1989; Basser and Pierpaoli, 1996; Inglese et al., 2005). The injuries are seldom visible on computed tomography (CT) and conventional MRI scans, besides the fact that not many approaches are available to assess the WM damage (Adams et al., 1985). Previous studies have suggested that the DAI is only visible by using advanced neuroimaging techniques that are able to distinguish microstructural tissue damages (Smith et al., 2019; Douglas et al., 2019). Diffusion tensor imaging (DTI) is an advanced MRI technique that detects changes in water diffusion in the brain due to microstructural pathology, or in other words, assesses WM structural integrity (Douglas et al., 2015). WM connectivity and integrity changes can be quantified using several measures of diffusion anisotropy along specific fiber tracts between different brain regions. Fractional anisotropy (FA) measures the directionality of water diffusion or the amount of diffusion asymmetry within a voxel. Mean diffusivity (MD) quantifies the total water diffusion, regardless of its direction (Uddin et al., 2019). Mode of anisotropy (MA) is a measure recently developed to help differentiate the local diffusion profile between a planar disc-like (as in fiber crossing) shape and a linear, cylindrical shape (as in unidirectional converging fibers bundle)(Ennis and Kindlmann, 2005).

DTI approach has been quite promising in evaluating WM DAI. Previous studies have shown that damaged WM due to TBI causes increased MD and reduced FA in WM (Shenton et al., 2012). Moreover, DTI measures (including FA, MD, axial diffusivity (AD), radial diffusivity (RD)) have been reported to consistently correlate with neurocognitive behaviors after TBI (Niogi et al., 2008; Newcombe et al., 2011; Wozniak et al., 2007; Hashim et al., 2017; Veeramuthu et al., 2015; Spitz et al., 2013). For example, in (Spitz et al., 2013), the relationship between WM integrity and cognitive functions including memory, information processing speed, and executive functions were evaluated using DTI-based FA measure, wherein a reduced

FA was associated with poor cognitive measures using tract-based analysis. Although all these studies are suggesting that DTI measures are able to investigate the structural cause of neurocognitive deficits after TBI, a few studies have explored the association between the motor impairments and WM integrity in TBI populations (Caeyenberghs et al., 2010b, 2011; Drijkoningen et al., 2015a). In these studies, lower WM anisotropy in some brain ROIs such as the cerebellum, corticospinal tract, and posterior thalamic radiation was correlated with lower postural performances. DTI measures will be used evaluate the associations between changes in WM structure and balance and related functional connectivity deficit in TBI.

#Study outline: Finally, explain what's the significance of our proposed approach in a few lines#

The objective of this work is to study the graph-theoretical properties in a functional connectivity graph computed from the source-constructed EEG during a balance perturbation task in TBI. To the best of our knowledge, this is the first study to report the changes in functional integration and segregation during a postural control task in TBI. Also, another key contribution is the investigation of the association between the structural and functional connectivity during a balance task in TBI and its relation to balance outcomes.

Materials and Methods

Participants:

In this study, 18 individuals with a chronic TBI and 18 healthy controls (HC) with no history of brain injury participated. Participants were recruited through our in-house patient information management system and Kessler Institute for Rehabilitation. Upon careful visual inspection of the raw EEG data, we excluded the data from 4 participants (1 TBI, 3 HC) as they were too noisy. Also, not every participant underwent the MRI scan, thus we were limited to the DTI data from 12 TBI and 9 HC. Summary of the demographics is presented in Table I. Inclusion criteria for participants are they must be- 1) aged between 18-65 years, (2) diagnosed with a TBI at least 6 months ago (or be a healthy control), (3) medically stable in the past 3 months, (4) be able to stand unsupported for 5 minutes. Exclusion criteria are as follows- (1) history of lower-limb injury in the past 90 days, (2) history of medication that could affect the balance/muscle coordination, (3) have any additional orthopedic, neuromuscular or neurological conditions that could affect balance (4) have a penetrating TBI, and (5) have a history of previously diagnosed balance impairments (prior to TBI). The subject demographics and disease characteristics are summarized in Table 1.

Data Acquisition:

Table 1: Summary of Participant Characteristics

Parameters	TBI	HC	p-value
N	12	9	
Severity	Mild = 2; Moderate = 4; Severe = 6	NA	NA
Years post injury (mean, range)	12.05, [1.67,57.87]	NA	NA
Age (mean ± std)	48.5 ± 12.03	48.55 ± 10.02	0.99
Gender (M/F)	10/2	5/4	
Height in cm (mean ± std)	179.01 ± 7.03	172.79 ± 7.47	0.065
Weight in kg (mean ± std)	87.14 ± 19.61	78.24 ± 18.12	0.3

Figure 2: A representative subject standing on the dynamic posturography platform used in the study

MRI Data Acquisition and Processing:

A high-resolution T1-weighted image using MPRAGE sequence was acquired using the Siemens Skyra 3T scanner (Erlangen, Germany) at Rocco Ortenzio Neuroimaging Center at Kessler Foundation. The following settings were used in the whole-brain volumetric acquisition with the following specifications: 1-mm isotropic

voxel resolution, TE=3 ms, TR=2300 ms, 1-mm thick 176 slices, Field of View (FOV) 256x256 mm^2.

A diffusion-weighted (DW) dataset were collected with 64 noncollinear DW gradients with b=1100 s/mm^2 and eight b=0 images, matrix size=128×128, FOV=256×256 mm^2, TE=75 ms, TR=9000 ms, isotropic voxel dimensions=2mm, and 66 slices. The gradient-echo field map images were acquired to correct for geometrical distortion caused by susceptibility artifacts. The image processing was performed using the FSL 6.0 toolbox that includes: 1) skull stripping using the Brain Extraction Tool (BET), 2) eddy current correction, 3) DTI-FIT diffusion tensors using FDT (FMRIB's Diffusion Toolbox, http://www.fmrib.ox.ac.uk/fsl, Oxford, UK). The generated results include parametric maps of DTI metrics, including mean diffusivity(MD), mode of anisotropy (MA), and fractional anisotropy (FA). Finally, the global FA, MD, and MO values for each subject were obtained by averaging the corresponding FA, MD, and MA values of the voxels in the skull-stripped mask, using FSL maths (Smith et al., 2004). Also, the voxel-wise statistical analysis of the FA images was carried out using the Tract-based spatial statistics (TBSS) (Smith et al., 2006) tool from FSL. First, all the FA data across subjects were aligned to the high-resolution FMRIB58_FA standard space image using the nonlinear registration (Andersson et al., 2007; Smith et al., 2007), and subsequently mapped into a 1x1x1mm standard space. This data was then averaged across subjects to obtain the group's mean FA image, from which the mean FA skeleton was derived as a reflection of the center of fiber bundles. Finally, the subject-specific FA images are projected onto the mean FA skeleton to perform a between-group analysis with the FSL function "randomize" and using the threshold-free cluster enhancement (TFCE). In addition to FA, diffusivity maps based on MD and MA were created as described above.

Postural Data Acquisition and Processing:

To study the effects of unpredictable balance perturbation, we used the computerized dynamic posturography (CDP) platform (NeuroCom Balance Master, NeuroCom Intl, Clackamas OR) as shown in Fig. 2. Henceforth, we use the term "CDP platform" and "balance platform" interchangeably. The participants were asked to stand on the balance platform and they were subject to five blocks of random unpredictable perturbations in the anterior (forward) and posterior (backward) sinusoidal perturbations at 0.5Hz, (two cycles for a total of 4s duration) at low (0.5cm) and high (2cm) amplitude with an inter-trial separation of 4-8s. Thus, there are 2x2 combinations of perturbation − anterior and posterior (direction), low and high (amplitude). We measured the center of pressure (COP) time series from the ground reaction force data. The COP data were epoched, low-pass filtered (10Hz), detrended, and averaged across trials and conditions for each subject. The COP displacement was computed as the cumulative distance traveled by the trial average COP in the anterior/posterior direction for the first 2s of the balance perturbation. In this article, our analysis was limited to the high amplitude perturbation in the posterior direction which led to greater instability across all subjects.

EEG Data Acquisition and Preprocessing

Throughout the duration of the task, the brain activity was recorded using the 64-channel EEG (ActiCAP BrainAmp standard, Brain Products®, Munich, Germany) positioned according to the International 10-20 systems where the electrode änd "AFz" serve as the common reference and ground respectively@"FCzänd "AFz" serve as the common reference and ground respectively. EEG data were sampled at 500Hz and the skin-electrode contact impedance was ensured to be below 20k ohms by the application of electrode gel. The EEG electrode positions were 3D digitized using Brainsight® navigation system.

Data processing:

EEG Data preprocessing

EEG recordings were analyzed offline using EEGLAB toolbox (Delorme and Makeig, 2004). The raw EEG signals were first downsampled to 250Hz, followed by band-pass filtering between 1Hz and 50Hz using a

4th order Butterworth filter. Thereafter, the line noise was removed using the Cleanline plugin for EEGLAB; artifact-contaminated channels and noisy continuous-time segments were removed using the Artifact Subspace Reconstruction (ASR) plugin for EEGLAB (Mullen et al., 2015). The parameter for ASR to reconstruct the high variance subspace was set as 20 based on the findings reported in (Chang et al., 2020). Subsequently, we performed the Independent Component Analysis (ICA) via extended Infomax algorithm (Makeig et al., 1996). The resulting ICs, presumably originated from the following physiological or miscellaneous sources—brain, muscle, eye, line noise, channel noise, heart, or other—were labeled accordingly with the ICLabel plugin in the EEGLAB toolbox (Pion-Tonachini et al., 2019). The ICLabel is a machine learning approach, which has been trained to classify the ICs derived from EEG data based on several characteristics such as spectral properties, brain topography. Furthermore, to validate the ICs supposedly generated by neural sources, DIPFIT tool (available in EEGLAB) was used that localizes the dipoles within the brain volume (Delorme et al., 2012),(Oostenveld and Oostendorp, 2002) In our study, we only retained the ICs that were (1) identified as 'Brain' by the ICLabel plugin and (2) having a residual variance of <15% after localization by DIPFIT modeling. Although we used the ICLabel for automating the labeling of ICs, we also visually inspected whether the characteristic topography and spectral properties of ICs corroborated with their respective labels. Once the ICs were selected, we used the back-projected sensor EEG for source localization.

EEG Source localization

EEG Source Localization (ESL) allows one to study the cortical dynamics using the underlying cortical sources estimated from the sensor-space EEG (Michel and Brunet, 2019; Shenoy Handiru et al., 2018). The ESL problem is mathematically formulated as:

$$\mathbf{X} = \mathbf{L}_f \mathbf{S} + \boldsymbol{\epsilon} \tag{1}$$

where $\mathbf{X} \in \mathbb{R}^{N \times T}$ represents the sensor-space EEG with N channels (or sensors) and T timepoints, $\mathbf{L}_f \in \mathbb{R}^{N \times M}$ denotes the lead-field matrix that projects M sources $(M >> N)$ onto the sensor-space, $\mathbf{S} \in \mathbb{R}^{M \times T}$ denotes the cortical source time series, and $\boldsymbol{\epsilon} \in \mathbb{R}^{N \times T}$ denotes the measurement noise. The two unknowns, $\mathbf{L}_f$and $\mathbf{S}$, are estimated using (1) forward modeling and (2) inverse modeling, respectively. Forward modeling is done to compute the volume conductor model which realistically approximates the electromagnetic field propagation through different layers in the head model (scalp, skull, cerebrospinal fluid, grey matter, and white matter). As the sensor-space EEG is only a projection of the true cortical activity, one needs to compute a realistic individual head model for which we use the subject-specific anatomical data. To this end, we used a subject-specific T1-weighted MRI and 3D digitized EEG positions to compute the head model by means of the 3-layered Boundary Element Method (BEM) (Fuchs et al., 1998; Gramfort et al., 2010). The default settings of conductivity values in OpenMEEG software were used for 3-layered BEM (scalp =1, skull = 0.0125, brain = 1) (Gramfort et al., 2010). Once we obtained the head model, $\mathbf{S}$ was computed using an inverse modeling algorithm named sLORETA (standardized Low Resolution Electromagnetic Tomography) (Pascual-Marqui, 2002). All the aforementioned steps were implemented using Brainstorm software (Tadel et al., 2011).

The EEG data processing pipeline is summarized in the block diagram shown in Fig. 3.

Functional connectivity: Imaginary part of coherence

We denote the imaginary part of coherence as $\mathrm{Im}(\underline{\mathbf{\Gamma}})$ with $\underline{\mathbf{\Gamma}} \in \mathbb{C}^{U \times U \times V}$ being a three-way tensor, where U and V are the number of ROIs and frequency bins of interest, respectively. The phase synchrony between two signals i and j can be measured using $\mathrm{Im}(\underline{\mathbf{\Gamma}}(i, j, :))$, which has been employed in (Nolte et al., 2004) to represent the statistical similarity between two brain sources derived from EEG. It is desirable to use $\mathrm{Im}(\underline{\mathbf{\Gamma}})$

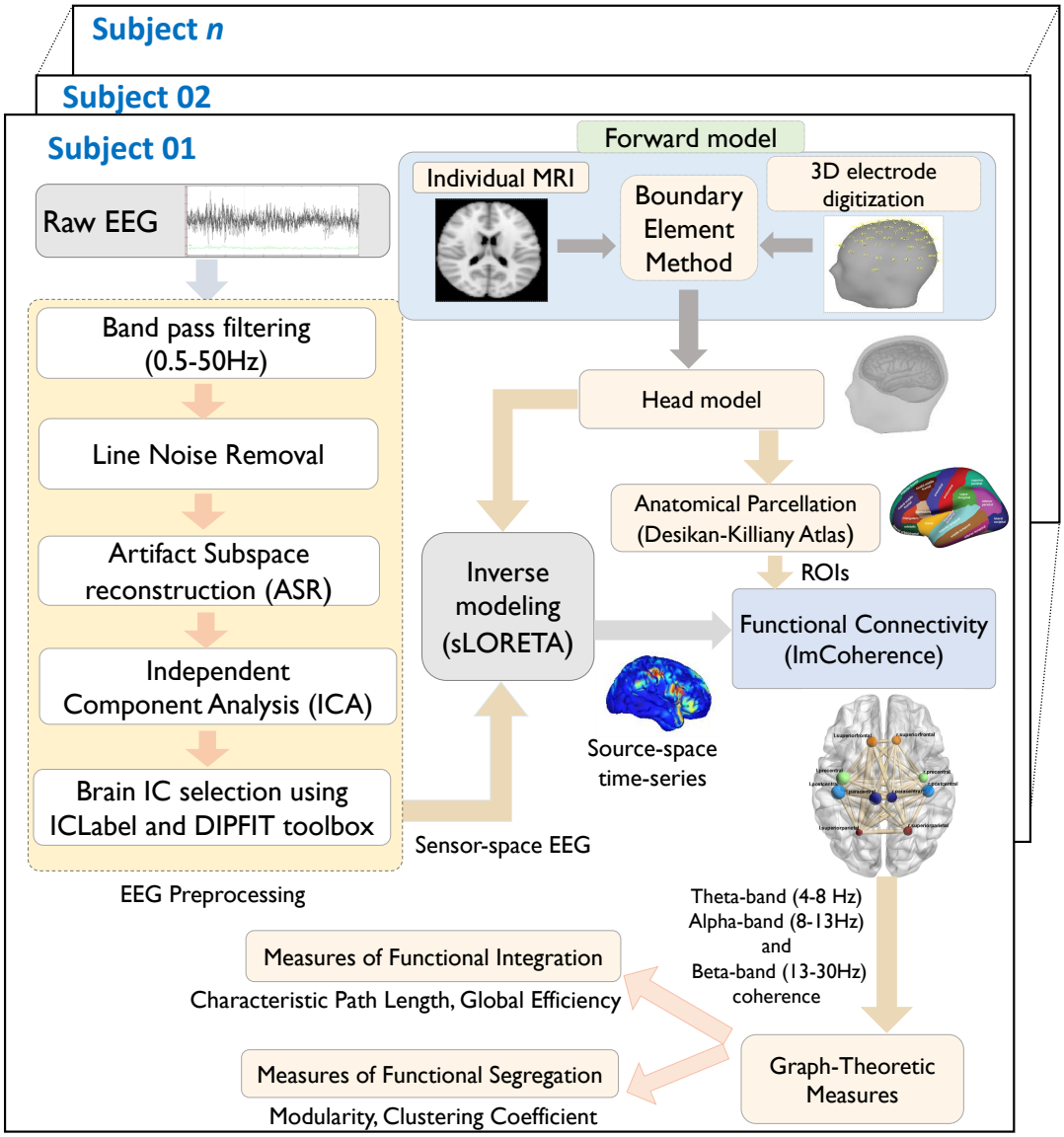

Figure 3: Block diagram of the EEG processing pipeline

since one can easily isolate the entries arising due to the volume conduction effect (VCE), i.e., the non-zero values of the tensor guarantee non-zero delays. In other words, the entries of $\mathrm{Im}(\underline{\mathbf{\Gamma}}(i,j,:)) \neq 0$, only when the respective frequency components of i and j are statistically independent. Therefore, the non-zero entries of $\mathrm{Im}(\underline{\mathbf{\Gamma}}(i,j,:))$ imply that there is no time-lagged interaction between the corresponding frequency bins of i and j due to VCE. Note that i and j are the time series generated by the brain ROIs of interest in our context.

Let us consider the kth segment of the ith time series as $x_{i,k}$ and its corresponding Fourier Transform as $X_{i,k}(f)$ at frequency f. The cross-spectral matrix $S_{i,j}(f)$ is then computed as (Nolte et al., 2004).

$$S_{i,j}(f) = \frac{1}{K}\sum_{k=1}^{K} X^{*}_{i,k}(f)\, X_{j,k}(f) \tag{2}$$

$$\underline{\mathbf{\Gamma}}(i,j,f) = \frac{S_{i,j}(f)}{\left[S_{i,i}(f)\, S_{j,j}(f)\right]^{1/2}} \tag{3}$$

where * refers to the complex conjugate. Finally, for the neural activity during the rest (t = -2s to 0s) and task (t = 0s to 2s) period, Im($\underline{\mathbf{\Gamma}}$) was computed and averaged across frequencies to obtain coherence measures for the theta band (4-8Hz), alpha-band (8-13Hz) and beta-band (13-30Hz), given their distinct role in sensorimotor function (Omlor et al., 2011; Buchholz et al., 2014).

Graph-Theoretic measures:

We can recall that the *functional segregation* informs us about the local network properties such as how densely connected are the sub-networks (or *modules*) (Newman, 2006) (Fig. 1A). Alternatively, the *functional integration* encapsulates the information about the ease of interaction between these sub-networks (Fig. 1B). The following graph-theoric measures to characterize the functional segregation and integration of the network were computed for both alpha- and beta-band connectivity. The weighted rather than the binary definition of the connection or edge between nodes are used, which is defined as the normalized connectivity strength with values between 0 and 1 (Rubinov and Sporns, 2010).

Measures of Functional Integration:

Global Efficiency (E_{global}): describes how well connected is the neighborhood of a node. It is a measure of the efficiency of information transfer among all pairs of nodes in the graph,

$$E_{\text{global}} = \frac{1}{N(N-1)}\sum_{i,j\in G}\frac{1}{d_{i,j}} \tag{4}$$

Where, N denotes the number of nodes in the graph G and $d^{w}_{ij} = \Sigma_{a_{uv}\in g^{w}_{i\leftrightarrow j}} f(w_{uv})$ denotes the shortest weighted path length between the nodes i and j in Graph G computed using the Djikstra's algorithm. $g^{w}_{i\leftrightarrow j}$ corresponds to the shortest weighted path between the nodes i and j and $f(w_{uv})$ denotes the mapping from connection weight to the path length (in this case, $f(w_{uv}) = (w_{uv})^{-1}$. In the context of brain connectivity, w_{uv} is the imaginary coherence value measured between the nodes u and v. Greater global efficiency would reflect overall more direct communication i.e. shorter path length between nodes.

Measures of Functional Segregation:

Modularity (M) is a measure of functional segregation that describes the *community structure* of a network (Newman, 2006). It compares the number of connections within *modules (or sub-networks)* to the number of connections across *modules.* Although there are different ways to compute the modularity, here we used Newman's algorithm as provided in the BCT toolbox (Rubinov and Sporns, 2010). The modularity score Q^{w} for a weighted connection matrix can be computed as below:

$$Q^{w} = \frac{1}{l^{w}}\sum_{i,j\in N}\left[w_{ij} - \frac{k^{w}_{i}k^{w}_{j}}{l^{w}}\right]\delta_{m_i m_j} \tag{5}$$

where, l^w is the sum of all weights in the given network (i.e. $l^w = \sum_{i,j} w_{ij}$). k_i^w and k_j^w denotes the weighted node degree of node i and j respectively (i.e. $k_i^w = \sum_{j \in N} w_{ij}$). m_i and m_j define the module containing the node i and j respectively. $\delta(c_i,\ c_j)$ defines the community structure i.e. $\delta_{m_i m_j} = 1$, if both nodes (or vertices) 'i ' and 'j ' belong to the same community.

Statistical Analysis

Data were confirmed for normality using visual inspection and Shapiro-Wilk test with a significance level of $\alpha = 0.05$. We performed the two-sample t-test to compare the differences in demographics characteristics (Age, Height, and Weight) and the COP displacement. As the normality assumption was not met, we performed a non-parametric statistical test (Wilcoxon ranksum test) for comparing the Berg Balance Scale –(BBS) across groups. To investigate the cortical regions involved during the balance perturbation task, we ran a parametric statistical test (student's t-test) at the population level in TBI and HC to identify significant voxel differences between the task period (t = 0s to 2s) and rest period (t = -2s to 0s). Because of the multiple comparisons, the correction for False Discovery Rate (FDR) was done using the Benjamini-Hochberg procedure with the significance value set at α=0.01.

Each imaginary coherence value between any two nodes (or ROIs) was tested for its statistical significance using Schelter's approach (Schelter et al., 2006) as implemented using bst_cohn() function in the Brainstorm toolbox.

The data being normal or pseudo-normal, we performed two-way repeated-measures analysis of variance (2x2 RMANOVA) using a general linear model, to compare the graph metrics across groups (TBI vs. HC) and time (rest period between -2s and 0s and balance perturbation task period between 0 to 2s) for each frequency band. Whenever an overall significant effect was found, corresponding post-hoc analyses using a two-tailed t-test were performed to examine between-group differences at baseline and/or during the task, between-group changes over time, and/or changes within the group.

The effect sizes are reported using partial eta-squared (η_p^2) values. The statistical analyses related to ANOVA and t-test were performed with SPSS (version 26, IBM, NY, USA), with the significance level set at $\alpha < 0.05$.

Furthermore, to determine whether network measures are associated with the behavioral measures, we calculated the Pearson correlation. In the case of correlation analysis, we identified the influential data points using a commonly accepted criterion of cook's distance > 4/N (Cook, 1977).

Results and Discussion

Participants characteristics and balance outcomes

A two-tailed t-test revealed no significant differences in the baseline demographics (Age, Height, and Weight) characteristics, as shown in Table I. As shown in Fig. 4, the BBS in the TBI group (median = 51, IQR = [45,55]) scored significantly lower (Wilcoxon ranksum test: z = -3.42, p=0.000617) than healthy controls (median=56, IQR = [56, 56]). In contrast, the TBI group showed only a non significant trend (t=1.23, p=0.23) toward larger displacement in the COP (mean ± SD = 10.43 ± 4.13, 95% CI =[7.8108,13.0650]) as compared to healthy controls (HC) (mean = 8.49 ± 2.59, 95% CI = [6.4951, 10.4897]). As reflecting by the much larger standard deviation and as shown in Fig. 4, the TBI group shows a wider range of COP displacement from comparable to much larger values than healthy controls.

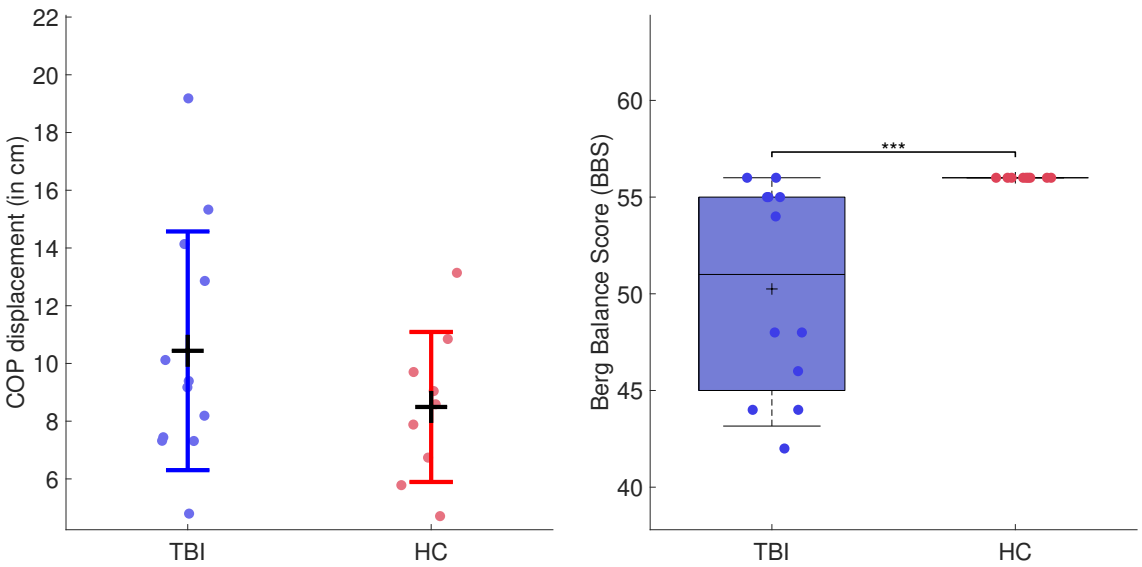

Figure 4: A group-level comparison of COP displacement (in cm) shown on the left. The black horizontal line on the COP plot marks the mean and the colored horizontal line marks the standard deviation. A group-level comparison of the Berg Balance Scale (BBS) is shown on the right as a boxplot due to its non-normal distribution. The horizontal line marks the median. The lower- and upper-hinge of the boxplot corresponds to the 25th and 75th quartile respectively. Statistical significance values are plotted as **(p<0.01), *(p<0.05) respectively.

Group differences in task-induced cortical activity during balance perturbation

Table 2 lists the key regions of interest that showed significant activity during the task as compared to baseline with the respective MNI coordinates as well as the number of significant voxels within each group. The spatial distributions of the significant voxels in different frequency bands are shown in Fig. 5.

Whole-brain functional connectivity

Fig. 6 shows the *non-normalized* functional connectivity and *non-normalized* node strength for each ROIs (defined as the sum of connectivity values to all other ROIs i.e. how strongly connected that ROIs are) based on source-space EEG coherence in the theta- and alpha-bands during the rest period as well as during the balance perturbation task in TBI and HC.

The two-way repeated-measure ANOVA conducted on Theta coherence-based network strength showed a main effect of *Time* (F(1, 19) = 43.4, p <10e-5, η_p^2 =0.70), but only a marginal non-significant *Group* effect (F(1, 19) = 3.42, p = 0.08, η_p^2 = 0.15), and no *Group*×*Time* interaction (F (1,19) = 0.05, p = 0.85, $\eta_p^2 = 0.002$). Within group contrast analysis using a within-group two-tailed t-test revealed a significant baseline to task change in network strength for TBI (t(22) = 4.13, p = 3.9e-5, rest: 426 ± 58, task: 663 ± 119). Likewise, the HC group also showed a significant change in network strength from baseline to task (t(16)= 4.03, p = 0.001 , rest = 479 ± 47, task = 730 ± 180). Between group contrast analysis revealed a greater network strength in HC compared to TBI at rest(t(19)=2.23, p=0.04).

When comparing the alpha-band network strength, two-way RMANOVA revealed a significant main effect of *Time* (F(1,19) = 10.8, p = 0.004, η_p^2 = 0.36) as well as *Group* (F(1,19) = 4.59, p = 0.045, η_p^2 = 0.19), but no significant *Group*×*Time* interaction (F(1,19) = 2.12, p = 0.16, η_p^2 = 0.10). Between group contrast analysis revealed a marginally lower network strength in TBI vs. HC (t(19) = 1.9, p = 0.07).

Table 2: MNI coordinates for contrast: perturbation task vs. resting period

Region Labels	TBI group					HC group				
	MNI coordinates					MNI coordinates				
	x	y	z	*t-value*	#voxels	x	y	z	*t-value*	#voxels
cingulate gyrus (Left)	-5	3	93	6.0611	36	15	-1	75	12.006	114
cingulate gyrus (Right)	0	-6	94	5.7049	36	2	-9	92	13.456	128
paracentral lobule (Left)	-11	0	119	5.9221	27	19	8	124	10.258	47
paracentral lobule (Right)	10	-4	92	4.856	25	12	-2	89	8.8717	61
post-central gyrus (Right)	-14	-14	119	4.941	29	7	-6	122	8.9055	92
pre-central gyrus (Left)	-6	4	122	5.5538	21	12	12	124	8.4168	68
superior frontal gyrus (Left)	30	1	117	4.5728	17	23	8	120	12.042	125
superior parietal gyrus (Left)	-23	22	110	5.1209	25	-30	14	118	5.5703	52
superior parietal gyrus (Right)	-27	-17	112	6.214	34	-20	-26	122	9.4985	67

Although the beta-band network strength was not significantly different within or between groups, we observed a close to significant higher network strength in HC as compared to TBI ($t(19) = 1.85$, $p = 0.08$). The results of the beta-band graph measures are included in supplementary materials. Overall, this shows the trend of globally weaker connectivity and weaker node strength in TBI compared to control.

Functional Graph Measures*:*

Two-way Repeated Measures Analysis of Variance (RMANOVA):

Global network measures of functional integration and segregation were measured using the Global Efficiency (E_g) and Modularity (M) respectively in different frequency bands (during the *rest* and balance perturbation *task*) for each group. The boxplot summary of the group-level comparison is shown in Fig. 7. The results for beta-band coherence connectivity were not significant, but for the sake of completion, they are included in the supplementary material.

The two-way repeated measure ANOVA was conducted on each of the graph measure separately. Theta coherence-based global efficiency showed a main effect of *Time* (F(1, 19) = 31.94, p <10e-5, η_p^2 =0.627), and a *Group* effect (F(1, 19) = 8.02, $p = 0.011$, η_p^2 =0.297), but no significant *Group* × *Time* interaction (F (1,19) = 0.0001, $p = 0.98$, $\eta_p^2 = 0.001$). As illustrated in Fig. 7, the within group post-hoc analysis revealed a significant baseline to task change in global efficiency for TBI (t(22) = 5.64, p = 10e-7, rest: .358 ± .036, task: 0.44 ± 0.036). Likewise, the HC group also showed a significant change in the global efficiency from baseline to task (t(16) = 4.07, $p = 0.001$, rest = 0.38 ± 0.023, task = 0.47 ± 0.06).

In the case of alpha coherence measure, for the global efficiency, the two-way repeated measure ANOVA showed a significant main effect of Group (F(1, 19) = 5.62, $p = 0.028$, $\eta_p^2 = 0.228$) but with no significant *Time* effect (F(1, 19) = 0.491, $p = 0.173$, η_p^2 =0.095) or *Group* × *Time* interaction (F (1,19) = 0.491, $p = 0.492$, η_p^2 =0.025). As illustrated in Fig. 7, the within group post-hoc analysis revealed no significant baseline to task change in global efficiency for TBI (t(22) = -0.7, $p = 0.49$, rest: 0.27 ± 0.029, task: 0.29 ± 0.055) and for HC (t(16) = -1.32, $p = 0.2$, rest: 0.40 ± 0.028, task: 0.42 ± 0.05). Given that the Global Efficiency failed the test of normality for TBI, we verified results obtained by running the non-parametric Wilcoxon test which similarly showed no significant change (z=-0.31, $p = 0.75$) from rest (median = 0.39 IQR = [0.36,0.4]) to task period (median = 0.39, IQR = [0.37,0.41]).

To investigate the task and group effect on functional segregation, the two-way repeated-measures ANOVA comparison was performed on the network modularity measures derived from different frequency bands. In case of theta coherence-based network modularity, we noticed a significant effect of time (Wilk's lambda

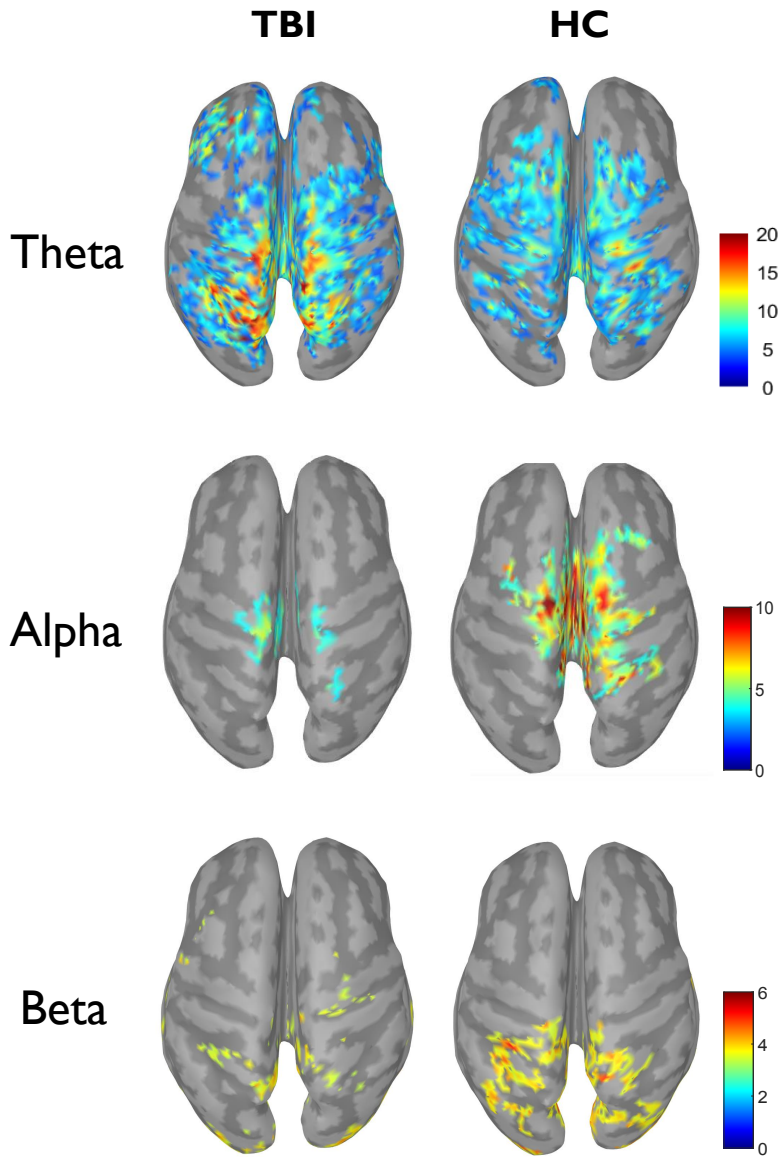

Figure 5: Spatial distribution of task-specific significant voxels mapped onto the cortex within each group. Parametric student's t-test is used to identify the voxels that are significantly different from the task period (t=0 to 2s) as compared to the resting period (t=-2s to 0s). FDR correction is with the significance level of α=0.01.

= 0.28, F(1, 19) = 48.6, p = 10e-6, η_p^2 =0.72), but no *Group* $\times$ *Time* interaction (F (1,19) = 0.024, p = 0.88, η_p^2= 0.001) and also there was only a marginal trend of main effect of *Group* (F(1, 19) = 3.03, p = 0.098, η_p^2 = 0.14). The post-hoc within-group analysis for modularity at rest vs. task within each group was also performed. We observed a significant difference from rest to task period within HC (t(16) = 3.30, p = 0. 0045, rest: .28 $\pm$ 0.03 task = .40 $\pm$ .09) but not for TBI (t(22) = 3.22, p = 0.003 , rest: 0.25 $\pm$ .03, task = 0.37 $\pm$.05).

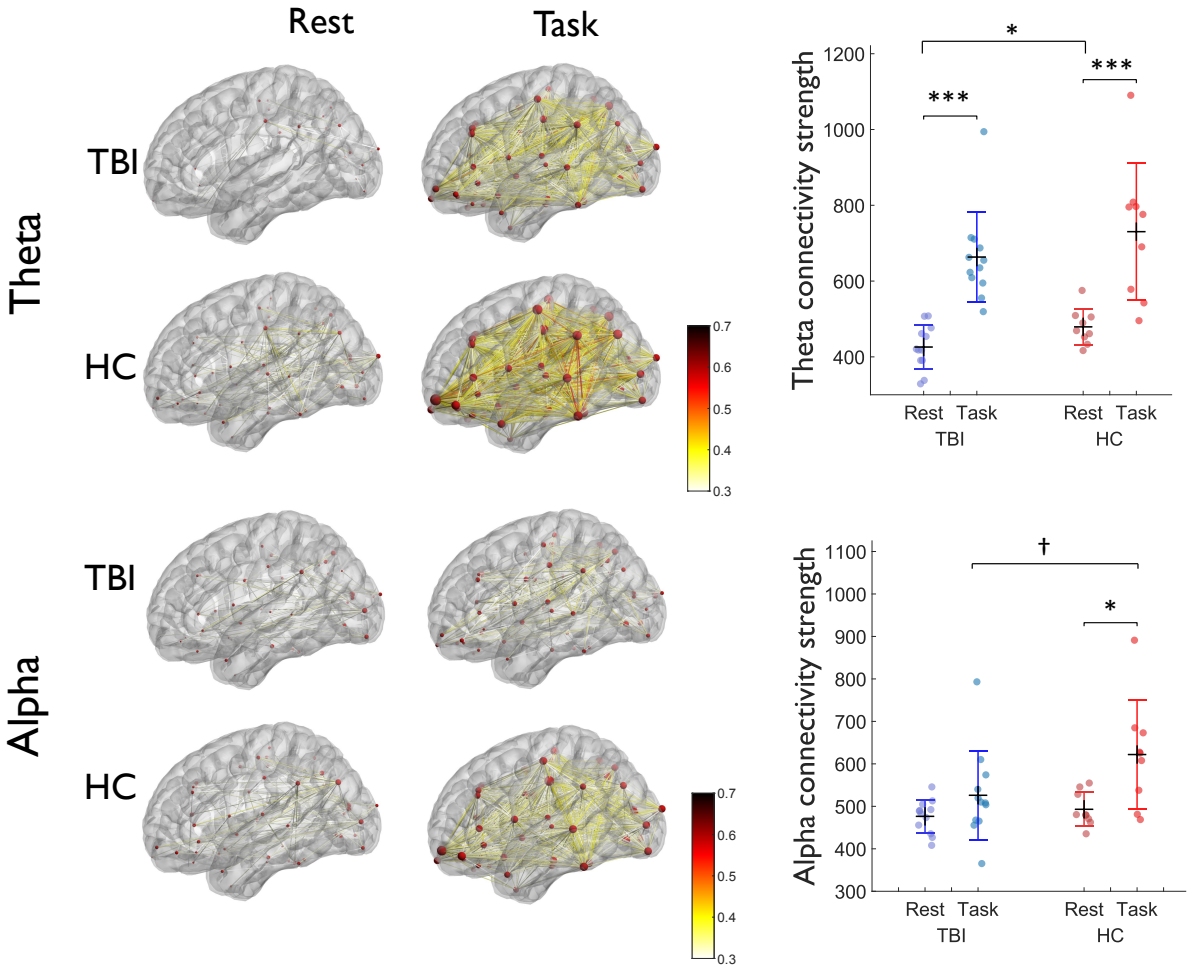

Figure 6: Whole-brain functional connectivity based on source-space EEG coherence in different frequency bands in each group (*TBI* and *HC*) across time periods (*rest* and *task*). Group-level connections are averaged and plotted as an edge between different ROIs anatomically parcellated using Desikan-Killiany Atlas. For better visualization, the connections are thresholded at edge weight = 0.3. Seed voxels of each ROI are indicated as spheres with a radius proportional to their node strength. On the right side, the boxplot comparison of network strengths during the rest vs. task period is shown for both the groups. Statistically significant differences are highlighted with asterisk * ($p < 0.05$), ** ($p<0.01$), *** ($p<0.005$), and marginally significant difference is highlighted with a † ($p<0.1$). Visualization of the cortical map is done with the help of BrainNet Viewer (Xia et al., 2013).

In case of alpha coherence-based network modularity, there was a significant effect of time ($F(1, 19) = 6.514$, $p = 0.019$, $\eta_p^2 = 0.255$) and *Group* × *Time* interaction ($F(1,19) = 4.696$, $p = 0.043$, $\eta_p^2 = 0.198$) but not of group ($F(1, 19) = 2.416$, $p = 0.137$, $\eta_p^2 = 0.113$). Indeed, as shown in Fig. 7, regions are functionally less segregated during the balance perturbation compared to rest for HC ($t(16) = 3.02$ $p = 0.008$, rest: 0.0465 ± 0.01, task: 0.03 ± 0.011) but not for TBI ($t(22) = 0.272$, $p = 0.788$, rest: 0.045 ± 0.011, task: 0.043 ± 0.011). This change in HC was found to be significantly greater than TBI ($t(19) = 2.167$, $p = 0.043$, 0.016 ± 0.012 vs. 0.001 ± 0.017 respectively). Intuitively this suggests that during the perturbation task,

more cortical areas (aka 'network node') are interacting with each other in HC, thus reducing the functional segregation, but not in TBI.

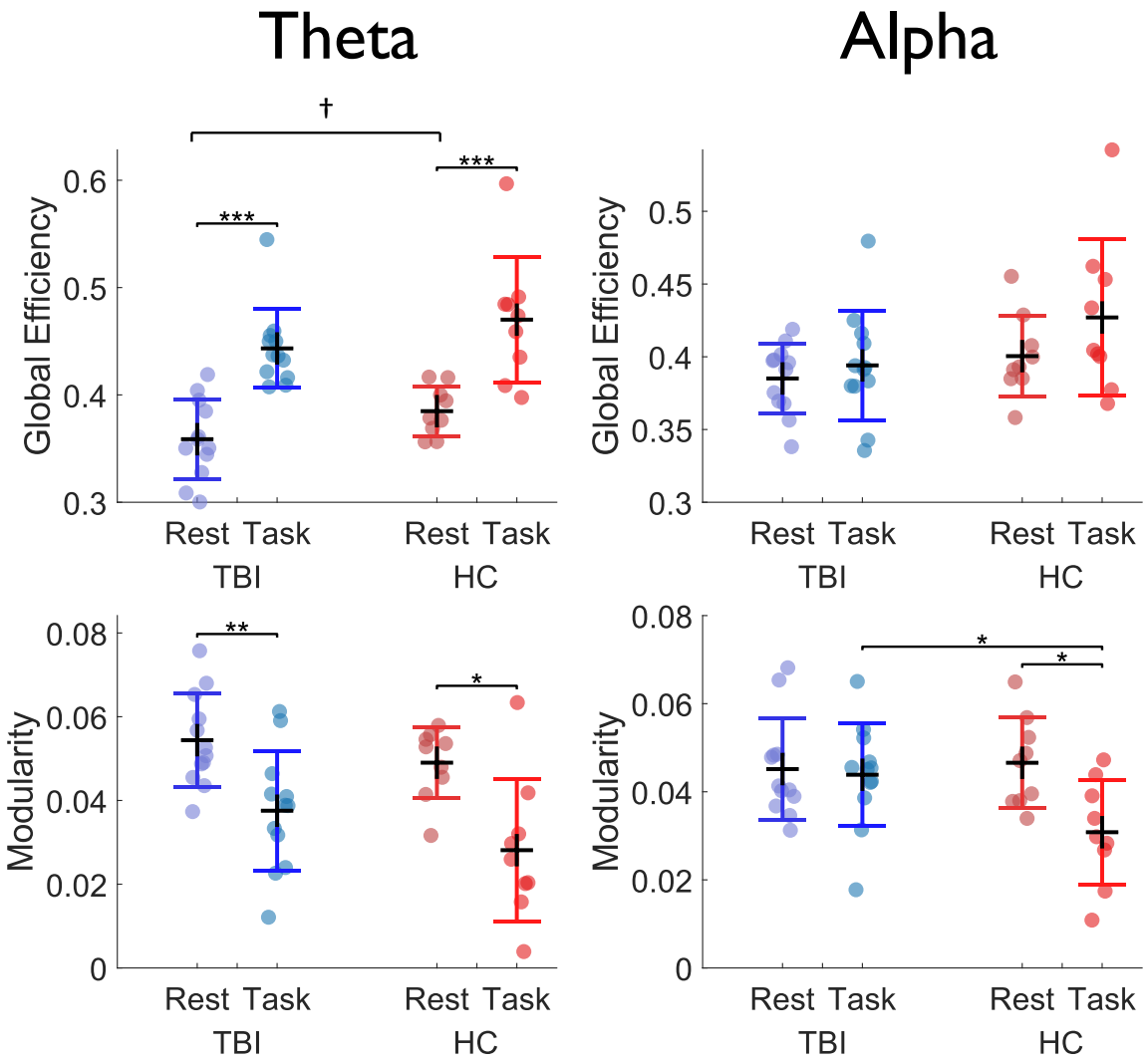

Figure 7: Group-level comparison of network measures of functional integration (top half) and functional segregation (bottom half) across frequency bands. The categorical scatter plot of the network measures during the resting state and during perturbation (task) within each group is shown above. Black horizontal line indicates the mean and the colored horizontal lines indicates the standard deviation. Statistically significant differences are highlighted with *($p<0.05$), **($p<0.01$).

Association between EEG graph-theoretic measures and behavioral measures

To explore the brain-behavioral relation, Pearson correlation coefficients between EEG graph measures in each of the frequency band and behavioral measures (i.e., COP displacement (in cm) and Berg Balance Scale

(BBS)) were calculated. To avoid spurious results given the small sample size, any outlier with a strong influence on the correlation based on the cook's distance D > 4/N criteria (Cook, 1977), was removed. Both results with and without outliers are reported for completeness (Fig. 9 (a)). None of the correlations survived the False Discovery Rate (FDR) correction for multiple comparisons, but the following significant associations were found when uncorrected. We observed a significant correlation ($r = 0.62$, $p = 0.03$ without and r=0.77, p=0.01 with outliers) between the theta-band modularity and the COP displacement in the TBI group (Fig. 9 (a)). Also, theta-band modularity was shown to be negatively correlated with the Berg Balance Scale (r = -0.74, $p = 0.01$). Finally, the beta-band network strength was positively correlated with the BBS (higher the network strength, better balance score) but only when the outlier was removed ($r = 0.7$, $p = 0.02$ with and $r = 0.51$, $p = 0.09$ without outlier).

Group differences in global DTI measures

Changes in structural networks were assessed by performing group comparison of the global measures of DTI as fractional anisotropy (FA), mean diffusivity (MD), and mode of anisotropy (MA) computed for the whole brain of each participant. All three metrics showed significant differences in structural connectivity between TBI and HC subjects (see Fig. 8). More specifically, the global FA measure is significantly lower ($F(1,19) = 10.7$, $p = 0.004$) in TBI (mean=0.234 ± 0.015, 95% CI: [0.225,0.243]) than in HC (mean = 0.256 ± 0.013, 95% CI: [0.247,0.265]). MD values are significantly higher ($F(1,19) = 6.68$, $p = 0.018$) in TBI (mean=0.0011 ± 0.00008, 95% CI:[0.0011,0.0012]) than HC group (mean=0.001 ± 0.00008, 95% CI: [0.001,0.0011]). Also, as shown in Fig. 8, significant difference ($F(1,19) = 5.66$, $p = 0.028$) was observed for the third DTI metric, the global MA measure between TBI (mean=0.214 ± 0.022, 95% CI: [0.202,0.227]) and HC (mean=0.236 ± 0.017, 95% CI: [0.225,0.247]).

To address the structural changes in brain white matter between groups, we conducted the voxel-wise analysis for the FA images using TBSS as shown in Fig. 8(c). Areas in red are regions where FA was significantly higher ($p = 0.02$) in HC than TBI, specifically in Corpus Callosum and Thalamus. No significant differences were observed between groups' comparison of MD and MA skeletons.

Association between DTI measures and behavioral measures

To explore the underlying association between white matter damage and balance, the correlation between DTI global metrics (FA, MD, and MA) and behavioral measures i.e. COP and BBS, in TBI patients were studied. There was a significant negative relationship between MD and BBS (r = -0.78, $p = 0.0043$ without and r = -0.64, $p = 0.02$ with outlier; Fig. 8 (b)) which is basically implying that higher MD values or more damaged brain tissues (more free diffusions) are correlated with lower BBS.

Association between global DTI measures and global EEG connectivity graph measures

To explore the underlying association between structural and functional connectivity graph metrics during postural control task, the correlation between each of the three functional graph metrics (Global Efficiency, Modularity, and Network Strength) and global DTI metrics (FA, MD, and MA) were analyzed using the Pearson correlation test. The significant correlations are shown in Fig. 9. Global fractional anisotropy values were significantly negatively correlated with the alpha-band network modularity (r = -0.65, $p = 0.03$ without and r = -0.59, $p = 0.04$ with outliers), and positively correlated with the global efficiency ($r = 0.59$, $p = 0.04$), and network strength ($r = 0.77$, $p < 0.01$ without and $r = 0.75$, $p = 0.01$ with outliers) (Fig. 9b). Although the beta-band network measures did not show any significant effects earlier in terms of the within-group and between-group differences, we observed the beta-band network strength was significantly associated with all the DTI measures in the TBI group (Fig. 9c). The beta-band network strength was positively associated

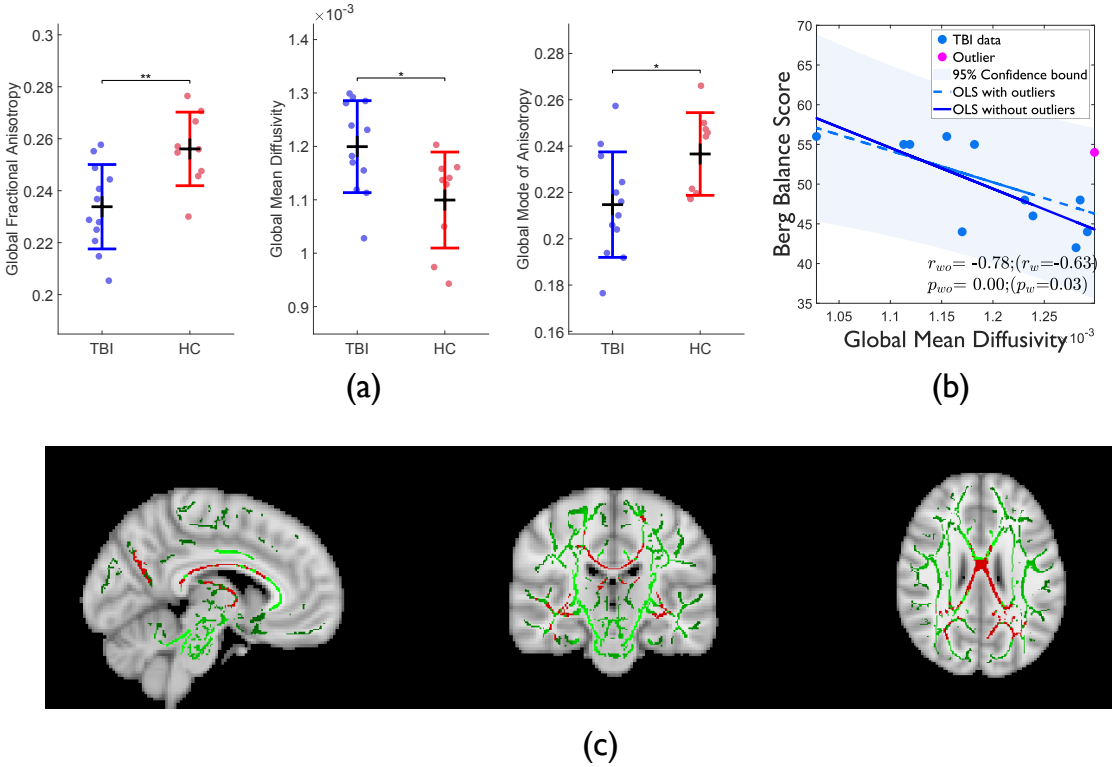

Figure 8: (a) Boxplots showing the differences in global DTI measures across groups. Statistically significant differences are highlighted with *(p<0.05), **(p<0.01). (b) Ordinary Least Squares Regression Plot of the association between the Berg Balance Scale score and global Mean Diffusivity. (c) Three views (sagittal, coronal, and axial) of significant differences in FA skeleton between TBI and HC group. The underlying image is the MNI152-T1 template, the green contour is the mean FA skeleton, and the red one shows the regions with significantly higher (p = 0.02) FA values in HC group compared to TBI.

with the global fractional anisotropy (r = 0.72, p = 0.01 without and r = 0.65, p = 0.02 with outliers) , global mode of anisotropy (r = 0.82, p = 0.001 without and r = 0.77, p = 0.003 with outliers), and negatively correlated with the global mean diffusivity (r = 0.71, p = 0.01 without and r = -0.64, p = 0.047 with outliers).

Overall these results suggest a relationship between abnormal white matter integrity and functional connections. In contrast, there were no significant correlations between the EEG network measures and DTI metrics in the HC group.

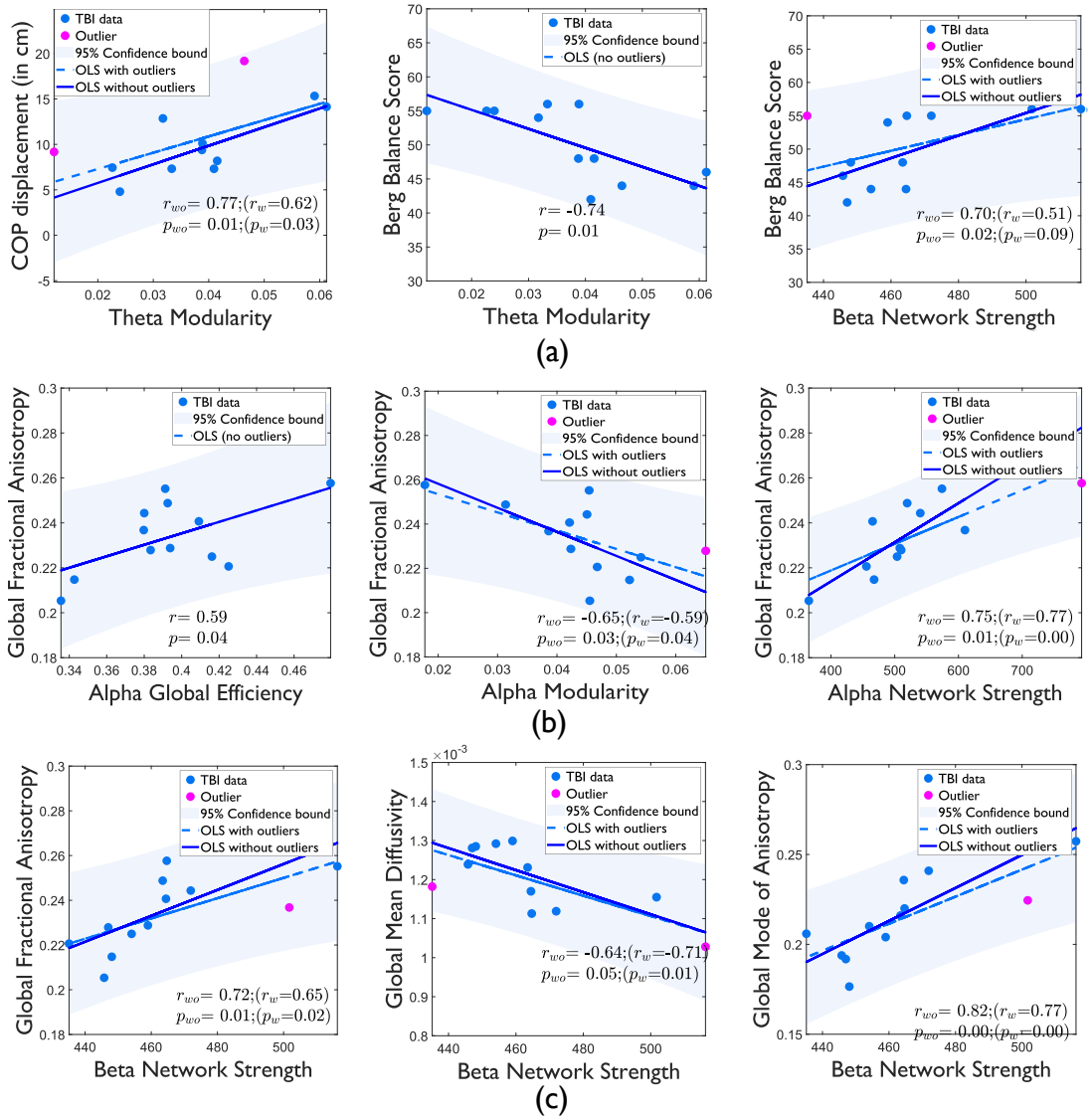

Figure 9: (a) Plots of the ordinary least squares regression correlation between the functional outcome measures (COP displacement/Berg Balance Scale in the Y-axis) and the global graph measures (X-axis). (b) The significant association between the global fractional anisotropy and alpha-band EEG graph measures, (c) The significant association between the global measures of structural integrity and the beta-band network strength during the postural control task across all subjects within the TBI group. The effect of outliers on the correlation is highlighted with two separate regression lines (*dashed line* when outliers are removed, *solid line* when the outliers are retained). r and p-values indicate the Pearson correlation coefficients and the significance level, respectively. r_w and p_w denote the correlation statistics when outliers are also taken into account; r_{wo} and p_{wo} denote the correlation statistics without outliers.

Discussion

In this study, we demonstrated the neural correlates of balance deficits using global and topological measures of functional and structural connectivity in the TBI population as compared to healthy controls. To the

best of our knowledge, this is the first time EEG based functional connectivity measures during a postural perturbation task in TBI and its association with the altered white matter integrity are reported.

Effect of TBI on balance

The widely used clinical measure of balance using the BBS shows an overall balance deficit in the TBI population compared to HC. However, there was a wide range of deficits with half of our sample scoring near the healthy maximal values of 56, while the other half below 48. A score of 45 has been traditionally considered the cut-off for a greater risk of falls (Berg et al., 1992), suggesting that half of the TBI population would have a greater risk of falls.

However, contrary to our hypothesis, we didn't find any significant group difference in balance deficit for the balance perturbation task with respect to the center of pressure displacement, i.e., body sway. This observation would suggest that overall, TBI managed to perform relatively well on the task compared to healthy controls. However, the larger standard deviation also highlights the broader range in performance on the task in TBI compared to HC, as well as the presence of a few TBI participants with more impaired postural control.

Effect of TBI on EEG brain connectivity and graph measures

Postural control is a complex task that relies on the proper functioning of distributed networks of visuo-sensory motor-related brain regions (Takakusaki, 2017). As TBI is often manifested as a diffuse axonal injury, the loss of white matter fiber tracts can disrupt the whole-brain network connectivity and functioning (Caeyenberghs et al., 2014). Graph theory can help identify alterations in the global brain connectivity organization (Griffa et al., 2013). Previous studies have shown that TBI disrupts the optimal 'small-world' architecture of the network (as often observed in the healthy population), affecting the optimal balance between local segregation within and global integration between specialized independent subnetworks(Griffa et al., 2013; Zhou, 2017; Imms et al., 2019). We seek to evaluate how TBI impairs this optimal integration/segregation balance at rest and during balance perturbation.

Resting results

Our graph-theoretical analysis revealed significantly reduced overall connectivity strength in the theta-band but not in the alpha or beta-band in the TBI group as compared to controls. This decreased connectivity strength in lower frequency bands is in agreement with (Boshra et al., 2020), who found lower delta and alpha connectivity in chronic mild TBI. (Cao and Slobounov, 2010) also observed decreased long-distance connectivity from frontal areas to other parts of the brain, but in the alpha band (they did not explore other frequency bands). However, this finding was for acute mild TBI 7-days after the concussion, which may explain discrepancies with our results. More generally, our resting state results contradict the hyperconnectivity hypothesis in TBI (Caeyenberghs et al., 2017) where an increase in connectivity strength or degree has been consistently found in the resting-state fMRI literature such as in (Caeyenberghs et al., 2012b; Diez et al., 2017). Hyperconnectivity is thought to result from an increase in local connection as a need to use detour paths around neurological disruption (Hillary and Grafman, 2017) or a compensatory response for the loss of long-range connections secondary to long-distance fiber tract damage (Venkatesan and Hillary, 2019). The brain imaging modality (e.g., EEG vs. fMRI) might be a factor confounding this observation as suggested in (Stam, 2014), especially given that TBI may alter the relationship between neural activity (EEG) and hemodynamics (fMRI) (Medaglia, 2017). Another explanation is that the current study included more severe and more chronic TBI, where it has been argued that more significant disruption may result or progress over time to hypoconnectivity due to structural resource loss (Hillary and Grafman, 2017) even though this theory has been questioned in TBI (Caeyenberghs et al., 2017).

Task effect

When looking at the task effect on brain activity, we observed an overall increase during the balance perturbation in both groups across frequency bands (Fig. 5). Interestingly, this activity increase was reduced in alpha and beta but was more significant for theta in TBI compared to HC, pointing to a different neural response to the increased task demand. It is also important to note that state changes in neural activity are observed in distinct brain regions with alpha band modulation seen over midline central (supplementary motor, lower-limb primary motor and sensory) regions, beta band over occipital and posterior parietal areas (visuo-sensory processing), and theta band over frontocentral and centro-parietal areas, suggesting distinct physiological roles of each frequency band.

Comparatively, the network connectivity strength increased from rest to task in both TBI and HC for theta, which saw the largest effects; HC only for alpha and marginally so (trend) for beta bands (Fig. 6). This resulted in a close to significant lower alpha network strength in TBI vs. HC during the task. The lower or lack of increase in alpha and beta network strength in TBI is consistent with the notion of impaired functional connectivity. Prior literature points to the evidence that the alpha oscillations play a role in coordinating the event-related cortical processes in such a way that they inhibit task-irrelevant neural structures but facilitates task-relevant neuronal networks (Klimesch et al., 2011). Furthermore, the function of alpha rhythms has been implicated in anticipatory sensorimotor events (Babiloni et al., 2014a; Talalay et al., 2018). Similarly, centro-parietal beta connectivity and activation have been implicated in attention and visuo-sensory processing to assist motor planning and execution (Chung et al., 2017). This result is consistent with our findings regarding increased connectivity and areas of the brain activated during the task.

Following our findings, theta-band activity has shown to increase in the frontocentral and centro-parietal regions significantly, mainly when there is an increasing balance task demand (Mierau et al., 2017; Solis-Escalante et al., 2019). Theta band synchronization within the frontoparietal areas plays a vital role in postural control by increasing attention and sensorimotor processing to improve error detection and processing for the proper planning and execution of postural movements (Mierau et al., 2017; Hülsdünker et al., 2015). Greater activation for TBI would suggest an increased attentional demand and/or more significant cortical effort to maintain balance due to more considerable postural instability, possibly as a compensatory response to reduced connectivity. Similarly, the impaired alpha and beta neural activation and network connectivity strength modulation, without a significant impact on the balance control performance in terms of body sway, would suggest that TBI participants can find a compensatory way to cope with the challenge from our specific balance task.

Integration

Our findings showed no significant between-group differences at rest in terms of the global network measures of integration, suggesting that the brain dynamics might not vary much due to pathology when there is no task demand. In contrast, we observed a significant increase in theta band (but not alpha- or beta-bands) global efficiency. This result is consistent with the findings in (Huang et al., 2016), where an increase in global efficiency, i.e., functional integration, was observed when participants were challenged to stand on a tilted as compared to a level-surfaced stabilometer. In general terms, the higher *weighted* global efficiency would imply stronger, more direct connections between nodes (Rubinov and Sporns, 2010). (Stam, 2014) suggests that this cortical reorganization is achieved likely through long *commissural* and a*ssociation fibers* linking different brain regions across- and within the hemisphere, respectively. This is consistent with the view that the neural synchronization at low frequency, including theta, facilitate distant regions' coordination, especially in response to increased task demands (Babiloni et al., 2017; Marek and Dosenbach, 2018). Interestingly, the marginal non-significant lower theta-band global efficiency in TBI than in HC at rest is no longer present during the task. We could speculate that the greater increase in theta activity in TBI may have been the manifestation of the need for a greater effort to increase network strength and global efficiency during the task to compensate for their lower values at rest.

Segregation

Concerning the functional segregation, we observed a decrease in modularity during the perturbation task

compared to rest in theta for both groups, in alpha for HC and none for the beta. Prior literature on the foot motor imagery task's neuroimaging suggested that the alpha rhythms are shown to engage in local information processing (akin to functional segregation) (Athanasiou et al., 2018). In contrast, beta rhythms are responsible for coordinating different processes (functional integration) (Athanasiou et al., 2018). In HC, the decrease in modularity during balance perturbation could be attributed to the increased complexity that necessitates the merging of network modules segregated during the resting state (Hearne et al., 2017). Neuroimaging of stabilometry studies substantiate our findings (Huang et al., 2016; Varghese et al., 2019). Relevant to our conclusions, Varghese (2016) postulated that the neighboring cortical areas of fronto-centro-parietal areas form new short-range connections to meet the increased demand and integration required to maintain balance control. As a result, the authors observed a decreased modularity during the perturbation-related task. We suspect that the minimal change in the modular network organization in alpha during the task to be caused by possible axonal damage in the TBI, disrupting task-specific connections.

Regarding the temporal dynamics of brain activity, we construe that these networks are functionally segregated or sparsely connected during rest; however, they communicate with each other depending on the demand for tasks. Balance control is a complex task requiring the proper coordination of a wide visuosensory-motor network (Takakusaki, 2017). The visuomotor and sensorimotor networks must quickly integrate the proprioceptive information from the lower limb (perturbation) in the current context of postural response to an external perturbation. As a responsive action, the supplementary motor area and associated systems try to initiate the upright posture control. Simultaneous efforts for both- functional integration and segregation are critical for efficient processing, termed 'small-world characteristics.' Our graph-theoretical analysis revealed significantly reduced overall connectivity strength and global efficiency compared to controls, consistent with the findings of altered small-world properties reported in (Cao and Slobounov, 2010; Pandit et al., 2013; Zhou, 2017).

Association between the EEG graph measures and the functional outcomes (COP & BBS)

While we did not notice any strong correlation between the global graph measures of EEG connectivity and the COP displacement or the berg balance scale score upon correction for multiple comparisons, we did notice theta modularity was positively correlated with the COP displacement and negatively correlated with the BBS. This suggests that the decrease in modularity would be associated with increased functional performance (i.e., lower COP or higher BBS). In a related experimental paradigm to ours, one of the recent studies exploring the modularity changes in the brain networks during sensorimotor learning (SMoL) task showed frequency-band specific changes (Miraglia et al., 2018). They also observed a negative correlation between theta-band modularity at rest and the percentage improvement of task performance, meaning that the lower the modularity at rest, the better the motor learning chance. In a resting-state functional connectivity study conducted by Scala et al. (Scala et al., 2019), global efficiency was negatively correlated with the COP displacement suggesting the increase in global efficiency would reflect better postural control.

Our correlation results should be taken with caution, given the weak association, which did not stand the FDR correction. Also, as with any correlational analyses, we caution the reader not to interpret this observation as causal.

Effect of TBI on structural damage

As previously mentioned, TBI can damage WM tracts due to diffuse axonal injury (DAI), potentially disrupting global functional network organization and, consequently, motor response. WM structural changes in TBI patients and healthy control were quantified using global DTI measures. Consistent with previous research studies (Douglas et al., 2015; Hashim et al., 2017; O'Phelan et al., 2018; Voelbel et al., 2012), we found a significant reduction in global WM microstructural integrity in TBI as reflected by lower FA and MA, and higher MD compared to controls. Reduced WM integrity and tract degeneration have consistently been reported in chronic TBI (Caeyenberghs et al., 2014; Hashim et al., 2017; Wallace et al., 2018). Following DAI, WM tract degeneration would lead to greater free water molecules movements, resulting in lower FA

and higher MD. Furthermore, reduced MA would signify more disc-like, less cigar-like shape water diffusion, i.e., more fiber crossing and less unidirectional fiber bundle (Douaud et al., 2011; Yoncheva et al., 2016), which could reflect the deterioration and thinning of WM tracts.

Furthermore, using TBSS, we compared the WM tracts in skeletonized maps in TBI and HC as a voxel-based group-level analysis for all three measures. Although global FA, MD, and MA were significantly changed in TBI, when these measures were registered on the standard space of major fiber tracts and projected onto the mean FA skeleton, significant group differences were found only in FA, not in MA or MD. In FA skeleton maps, the main regions affected were the thalamus and some parts of the Corpus Callosum, and parietal-occipital junction regions. This finding is not surprising knowing the role of the Corpus Callosum in the executive functions and processing speed and thalamus in the balance and other sensory-motor functions (Surgent et al., 2019). Future analyses should further investigate the regional and tract-based WM damage and their potential role in balance deficit and abnormal postural response to the perturbation task.

Association between DTI and BBS, and DTI and graph measures

Correlation analysis between the DTI measures and EEG graph-theoretic measures revealed that there was a consistent relation between the structural damage and less integrated, global synchronous connectivity during the task in TBI but not in HC. However, this particular observation was only in the alpha and beta bands. The global efficiency and network strength significantly correlated with the global fractional anisotropy in TBI. A similar observation was reported in a study conducted on Multiple Sclerosis patients. The long-range connectivity was shown to be associated with the fractional anisotropy, and the damage to these long-range connections was reflected in the global efficiency values (Rudie et al., 2013).

Moreover, the negative association between the Berg Balance Scale and mean diffusivity hints at overall white matter degeneration in poorer balance performance. Given our finding is based on the global mean diffusivity, our future work will investigate the diffusivity characteristics in more local tracts such as middle and inferior cerebellar peduncles, shown to be involved in postural control (Caeyenberghs et al., 2010c).

Regions of interest pertaining to postural control:

We postulate that new interventions for neuromuscular disorders should consider the individualized rehabilitative techniques that aid in the desirable neural plasticity. Given the brain's ability to engage in a compensatory mechanism especially post-injury, it would be important to explore how neural plasticity can be facilitated through techniques such as noninvasive brain stimulation. To this end, it is also important to understand which cortical regions are involved during the task of interest; pertaining to the balance impairment we want to know which regions are engaged during the postural control task in healthy controls more than TBI. As discussed earlier in the results section (Table 2), we observed task-specific cortical activation across both groups in the regions such as the cingulate gyrus, paracentral lobule, postcentral gyrus, precentral gyrus, superior parietal, and superior frontal gyrus. However, the number of group-level significant voxels of activation in the healthy controls was higher than TBI, indicating that brain injury may lower the level of neuronal activation. Such regions are of particular interest in the postural control model but are engaged with distinct objectives. Several studies corroborate our findings, wherein the cingulate gyrus (Goel et al., 2019) is shown to calibrate the postural response to a challenging continuous task.

Similarly, the role of the paracentral lobule in balance control is well-documented in the literature (Boisgontier et al., 2017; Diez et al., 2017; Goossens et al., 2019; Hagmann et al., 2008), along with the precentral gyrus (M1 region) (Taubert et al., 2016). The involvement of the superior parietal region in detecting postural instability is reported in (Slobounov et al., 2006) whereas the multisensory cortex activation was prominent in the somatosensory region (postcentral gyri) during lower-limb motor imagery tasks. The role of the prefrontal cortex and middle frontal cortex, which are part of the superior frontal cortex is demonstrated in (Mihara et al., 2008) as a response to an external perturbation of a posturography platform. In a recent study (Solis-Escalante et al., 2019), increased supplementary motor area (SMA) activation during the lower-limb tasks with higher postural demand highlighted the role of SMA in the preparatory-phase of

balance control in healthy volunteers.

Moreover, some of these regions also serve as a 'hub' of communication between other regions to facilitate functional integration thus substantiating the need for graph-theoretic analysis. Structural connectivity of whole-brain networks shows that these regions with a high degree of connectivity (superior frontal, cingulate gyrus, paracentral lobule) are located along the parasagittal line of the brain (Hagmann et al., 2008). It shows that the functional integration during the postural control is facilitated by the structural pathways (cortico-cortical axonal connections) that traverse these key regions of interest.

Our ongoing study that involves balance training using a stabilometry platform is aimed at identifying which of the brain regions aid in the improvement of balance control in TBI.

Limitations and future directions

We acknowledge that our study has some limitations, particularly with the small sample size. Also, there is another limitation concerning the heterogeneity within the sample population; this is particularly challenging in the TBI group because of the varying degrees of injury (mild/moderate/severe) not necessarily correlating with the motor deficits. However, we have tried our best to control for other factors such as age, height, and weight, which contribute to the postural control performance.

While we integrated information available from both task-based neuroimaging using the EEG and the structural imaging using DTI, it is worth highlighting that the functional connectivity between the time-series of two regions is often modulated by factors independent from the structural connectivity. Functional connectivity measure between two areas can be influenced by the third region with no direct fiber track in between, but still coordinated functionally via cortico-thalamocortical pathways (O'Reilly et al., 2017). We recommend that future studies must investigate the causal association between structural and functional connections.

About the graph-theoretic analysis, we admit we have not compared the graph metrics to the null model. In our defense, we highlight that the choice of the null model plays a critical role, and it can dramatically change the small-world properties of the network (Fallani et al., 2014). Moreover, the choice of FC measurement (e.g., correlation/coherence) can also affect the comparison concerning the null model. Nevertheless, unlike the correlation-based FC measurement, which often results in a spurious association between two regions, the coherence-based FC is tested for its statistical significance using Schelter's approach (Schelter et al., 2006). Incorporating these methodological details is our priority in the upcoming graph-theoretic studies.

In this study, our focus has been primarily on the global measures of EEG connectivity graphs. However, the underlying neural mechanisms of the postural control are too complex to summarize with a single statistical value. Depending on the research question, this can be either a strength or a weakness. In our current approach, we attempted to address whether we can identify a type of neural biomarker based on the EEG connectivity graph. While the global graph measures allow us to explore the association between the connectivity-based graph measures and the functional outcomes, it still does not answer questions related to the local characteristics of task-relevant networks. Notwithstanding this limitation, we did explore the local properties based on the weighted node strength and the significant cortical activity in the regions of interest to the postural control. Future work will examine the significance of these nodes in terms of local graph properties such as rich-club coefficient and centrality measures.

Conclusions

This is the first study investigating the brain network segregation and integration in a TBI group, especially during the task performed on a computerized stabilometric platform. The use of EEG-based FC measures and the DTI-based structural integrity measures helped us explain some of the underlying structural-functional mechanisms of postural control. The findings from EEG graph measures in TBI compared to the healthy

control group revealed some insights into the altered graph-theoretic properties in the brain functional networks. Also, we observed some of the measures of functional integration and segregation in TBI were associated with the measures of balance performance and structural integrity. These observations could pave the way for future research to identify cortical biomarkers of lower-limb motor deficits, thus assisting the clinicians, neuroscientists, and patients with neuromuscular disorders.

While ours is a study with a small sample size, we believe that our findings and inferences will provide directions to future studies on brain connectivity in TBI and other neuropathologies.

Data Availability

All the raw data are not publicly available due to IRB restrictions. However, the MATLAB scripts MATLAB scripts and the de-identified pre-processed EEG data supporting this study can be made available upon reasonable requests to the corresponding author.

Conflicts of Interest

The authors declare that there is no conflict of interest regarding the publication of this paper.

Funding Statement

The research was funded by a grant from the New Jersey Commission on Brain Injury Research (Grant #CBIR15MIG004).

Acknowledgements

References

JH Adams, D Doyle, DI Graham, AE Lawrence, and DR McLellan. Microscopic diffuse axonal injury in cases of head injury. *Med Sci Law*, 25:265–9, Oct 1985.

JH Adams, D Doyle, I Ford, TA Gennarelli, DI Graham, and DR McLellan. Diffuse axonal injury in head injury: definition, diagnosis and grading. *Histopathology*, 15:49–59, Jul 1989.

Didier Allexandre, Armand Hoxha, Vikram Shenoy Handiru, Soha Saleh, S. Easter Selvan, and Guang H. Yue. Altered Cortical and Postural Response to Balance Perturbation in Traumatic Brain Injury – An EEG Pilot Study. In *2019 41st Annual International Conference of the IEEE Engineering in Medicine and Biology Society (EMBC)*, pages 1543–1546. IEEE, jul 2019. ISBN 978-1-5386-1311-5. doi: 10.1109/embc.2019.8856645. URL https://ieeexplore.ieee.org/document/8856645/.

Jesper LR Andersson, Mark Jenkinson, Stephen Smith, et al. Non-linear registration aka Spatial normalisation FMRIB Technial Report TR07JA2. *FMRIB Analysis Group of the University of Oxford*, pages 1–22, 2007.

Alkinoos Athanasiou, Manousos A Klados, Charis Styliadis, Nicolas Foroglou, Konstantinos Polyzoidis, and Panagiotis D Bamidis. Investigating the role of alpha and beta rhythms in functional motor networks. *Neuroscience*, 378:54–70, 2018. doi: 10.1016/j.neuroscience.2016.05.044.

C Babiloni, A Brancucci, F Vecchio, L Arendtnielsen, A Chen, and P Rossini. Anticipation of somatosensory and motor events increases centro-parietal functional coupling: An EEG coherence study. *Clinical Neurophysiology*, 117(5):1000–1008, may 2006. doi: 10.1016/j.clinph.2005.12.028. URL https://doi.org/10.1016%2Fj.clinph.2005.12.028.

C Babiloni, Percio C Del, L Arendt-Nielsen, A Soricelli, GL Romani, PM Rossini, and P Capotosto. Cortical EEG alpha rhythms reflect task-specific somatosensory and motor interactions in humans. *Clin Neurophysiol*, 125:1936–45, Oct 2014a.

Claudio Babiloni, Claudio Del Percio, Lars Arendt-Nielsen, Andrea Soricelli, Gian Luca Romani, Paolo Maria Rossini, and Paolo Capotosto. Cortical EEG alpha rhythms reflect task-specific somatosensory and motor interactions in humans. *Clinical Neurophysiology*, 125(10):1936–1945, oct 2014b. doi: 10.1016/j.clinph.2014.04.021. URL https://doi.org/10.1016%2Fj.clinph.2014.04.021.

Claudio Babiloni, Claudio Del Percio, Susanna Lopez, Giancarlo Di Gennaro, Pier P. Quarato, Luigi Pavone, Roberta Morace, Andrea Soricelli, Giuseppe Noce, Vincenzo Esposito, Vittorio Gallese, and Giovanni Mirabella. Frontal Functional Connectivity of Electrocorticographic Delta and Theta Rhythms during Action Execution Versus Action Observation in Humans. *Frontiers in Behavioral Neuroscience*, 11, feb 2017. doi: 10.3389/fnbeh.2017.00020. URL https://doi.org/10.3389%2Ffnbeh.2017.00020.

PJ Basser and C Pierpaoli. Microstructural and physiological features of tissues elucidated by quantitative-diffusion-tensor MRI. *J Magn Reson B*, 111:209–19, Jun 1996.

André M Bastos and Jan-Mathijs Schoffelen. A Tutorial Review of Functional Connectivity Analysis Methods and Their Interpretational Pitfalls. *Frontiers in systems neuroscience*, 9(January):175, 2015. ISSN 1662-5137. doi: 10.3389/fnsys.2015.00175. URL http://www.ncbi.nlm.nih.gov/pubmed/26778976{%}5Cnhttp://www.pubmedcentral.nih.gov/articlerender.fcgi?artid=PMC4705224.

KO Berg, SL Wood-Dauphinee, JI Williams, and B Maki. Measuring balance in the elderly: validation of an instrument. *Can J Public Health*, 83 Suppl 2:S7–11, Jul 1992.

Matthieu P. Boisgontier, Boris Cheval, Sima Chalavi, Peter van Ruitenbeek, Inge Leunissen, Oron Levin, Alice Nieuwboer, and Stephan P. Swinnen. Individual differences in brainstem and basal ganglia structure predict postural control and balance loss in young and older adults. *Neurobiology of Aging*, 50:47–59, 2017. ISSN 15581497. doi: 10.1016/j.neurobiolaging.2016.10.024.

Rober Boshra, Kyle I Ruiter, Kiret Dhindsa, Ranil Sonnadara, James P Reilly, and John F Connolly. On the time-course of functional connectivity: theory of a dynamic progression of concussion effects. *Brain Communications*, 2(2), 2020. doi: 10.1093/braincomms/fcaa063. URL https://doi.org/10.1093%2Fbraincomms%2Ffcaa063.

Verena N Buchholz, Ole Jensen, and W Pieter Medendorp. Different roles of alpha and beta band oscillations in anticipatory sensorimotor gating. *Frontiers in human neuroscience*, 8:446, 2014.

Thomas A. Buckley, Jessie R. Oldham, and Jaclyn B. Caccese. Postural control deficits identify lingering post-concussion neurological deficits. *Journal of Sport and Health Science*, 5(1):61–69, 2016. ISSN 22132961. doi: 10.1016/j.jshs.2016.01.007. URL http://dx.doi.org/10.1016/j.jshs.2016.01.007.

K Caeyenberghs, A Leemans, M Geurts, T Taymans, CV Linden, BC Smits-Engelsman, S Sunaert, and SP Swinnen. Brain-behavior relationships in young traumatic brain injury patients: DTI metrics are highly correlated with postural control. *Hum Brain Mapp*, 31:992–1002, Jul 2010a.

K Caeyenberghs, A Leemans, M Geurts, T Taymans, Linden C Vander, BC Smits-Engelsman, S Sunaert, and SP Swinnen. Brain-behavior relationships in young traumatic brain injury patients: fractional anisotropy measures are highly correlated with dynamic visuomotor tracking performance. *Neuropsychologia*, 48:1472–82, Apr 2010b.

K Caeyenberghs, A Leemans, M Geurts, CV Linden, BC Smits-Engelsman, S Sunaert, and SP Swinnen. Correlations between white matter integrity and motor function in traumatic brain injury patients. *Neurorehabil Neural Repair*, 25:492–502, Jul 2011.

K. Caeyenberghs, A. Leemans, C. De Decker, M. Heitger, D. Drijkoningen, C. Vander Linden, S. Sunaert, and S.P. Swinnen. Brain connectivity and postural control in young traumatic brain injury patients: A diffusion

MRI based network analysis. *NeuroImage: Clinical*, 1(1):106–115, 2012a. doi: 10.1016/j.nicl.2012.09.011. URL https://doi.org/10.1016%2Fj.nicl.2012.09.011.

K. Caeyenberghs, A. Leemans, I. Leunissen, J. Gooijers, K. Michiels, S. Sunaert, and S. P. Swinnen. Altered structural networks and executive deficits in traumatic brain injury patients. *Brain Structure and Function*, 219(1):193–209, 2014. ISSN 18632653. doi: 10.1007/s00429-012-0494-2.

Karen Caeyenberghs, Alexander Leemans, Monique Geurts, Tom Taymans, Catharine Vander Linden, Bouwien C.M. Smits-Engelsman, Stefan Sunaert, and Stephan P. Swinnen. Brain-behavior relationships in young traumatic brain injury patients: DTI metrics are highly correlated with postural control. *Human Brain Mapping*, 31(7):992–1002, 2010c. ISSN 10970193. doi: 10.1002/hbm.20911.

Karen Caeyenberghs, Alexander Leemans, Marcus H. Heitger, Inge Leunissen, Thijs Dhollander, Stefan Sunaert, Patrick Dupont, and Stephan P. Swinnen. Graph analysis of functional brain networks for cognitive control of action in traumatic brain injury. *Brain*, 135(4):1293–1307, 2012b. ISSN 14602156. doi: 10.1093/brain/aws048.

Karen Caeyenberghs, Helena Verhelst, Adam Clemente, and Peter H. Wilson. Mapping the functional connectome in traumatic brain injury: What can graph metrics tell us? *NeuroImage*, 160:113–123, oct 2017. doi: 10.1016/j.neuroimage.2016.12.003. URL https://doi.org/10.1016%2Fj.neuroimage.2016.12.003.

C. Cao and S. Slobounov. Alteration of cortical functional connectivity as a result of traumatic brain injury revealed by graph theory, ICA, and sLORETA analyses of EEG signals. *IEEE Transactions on Neural Systems and Rehabilitation Engineering*, 18(1):11–19, 2010. ISSN 15344320. doi: 10.1109/TNSRE.2009.2027704.

Chi-Yuan Chang, Sheng-Hsiou Hsu, Luca Pion-Tonachini, and Tzyy-Ping Jung. Evaluation of Artifact Subspace Reconstruction for Automatic Artifact Components Removal in Multi-Channel EEG Recordings. *IEEE Transactions on Biomedical Engineering*, 67(4):1114–1121, apr 2020. ISSN 0018-9294. doi: 10.1109/TBME.2019.2930186. URL https://ieeexplore.ieee.org/document/8768041/.

Jae W. Chung, Edward Ofori, Gaurav Misra, Christopher W. Hess, and David E. Vaillancourt. Beta-band activity and connectivity in sensorimotor and parietal cortex are important for accurate motor performance. *NeuroImage*, 144:164–173, jan 2017. doi: 10.1016/j.neuroimage.2016.10.008. URL https://doi.org/10.1016%2Fj.neuroimage.2016.10.008.

Fabien Cignetti, Marianne Vaugoyeau, Leslie M. Decker, Marie-Hélène Grosbras, Nadine Girard, Yves Chaix, Patrice Péran, and Christine Assaiante. Brain network connectivity associated with anticipatory postural control in children and adults. *Cortex*, 108:210–221, nov 2018. doi: 10.1016/j.cortex.2018.08.013. URL https://doi.org/10.1016%2Fj.cortex.2018.08.013.

Jessica R. Cohen and Mark D'Esposito. The segregation and integration of distinct brain networks and their relationship to cognition. *Journal of Neuroscience*, 36(48):12083–12094, 2016. ISSN 15292401. doi: 10.1523/JNEUROSCI.2965-15.2016.

R Dennis Cook. Detection of influential observation in linear regression. *Technometrics*, 19(1):15–18, 1977.

Fabrizio De Vico Fallani, Floriana Pichiorri, Giovanni Morone, Marco Molinari, Fabio Babiloni, Febo Cincotti, and Donatella Mattia. Multiscale topological properties of functional brain networks during motor imagery after stroke. *NeuroImage*, 83:438–49, dec 2013. ISSN 1095-9572. doi: 10.1016/j.neuroimage.2013.06.039. URL http://www.ncbi.nlm.nih.gov/pubmed/23791916.

Arnaud Delorme and Scott Makeig. EEGLAB: An open source toolbox for analysis of single-trial EEG dynamics including independent component analysis. *Journal of Neuroscience Methods*, 134:9–21, 2004. ISSN 01650270. doi: 10.1016/j.jneumeth.2003.10.009.

Arnaud Delorme, Jason Palmer, Julie Onton, Robert Oostenveld, and Scott Makeig. Independent EEG sources are dipolar. *PLoS ONE*, 7(2), 2012. ISSN 19326203. doi: 10.1371/journal.pone.0030135.

Ibai Diez, David Drijkoningen, Sebastiano Stramaglia, Paolo Bonifazi, Daniele Marinazzo, Jolien Gooijers, Stephan P. Swinnen, and Jesus M. Cortes. Enhanced prefrontal functional–structural networks to support postural control deficits after traumatic brain injury in a pediatric population. *Network Neuroscience*, 1 (2):116–142., 2017. ISSN 24721751. doi: 10.1162/netn_a_00007.

Gwenaëlle Douaud, Saâd Jbabdi, Timothy E.J. Behrens, Ricarda A. Menke, Achim Gass, Andreas U. Monsch, Anil Rao, Brandon Whitcher, Gordon Kindlmann, Paul M. Matthews, and Stephen Smith. DTI measures in crossing-fibre areas: Increased diffusion anisotropy reveals early white matter alteration in MCI and mild Alzheimer's disease. *NeuroImage*, 55(3):880–890, apr 2011. doi: 10.1016/j.neuroimage.2010.12.008. URL https://doi.org/10.1016%2Fj.neuroimage.2010.12.008.

David B Douglas, Tae Ro, Thomas Toffoli, Bennet Krawchuk, Jonathan Muldermans, James Gullo, Adam Dulberger, Ariana E Anderson, Pamela K Douglas, and Max Wintermark. Neuroimaging of traumatic brain injury. *Medical Sciences*, 7(1):2, 2019.

DB Douglas, M Iv, PK Douglas, A Anderson, SB Vos, R Bammer, M Zeineh, and M Wintermark. Diffusion Tensor Imaging of TBI: Potentials and Challenges. *Top Magn Reson Imaging*, 24:241–51, Oct 2015.

D Drijkoningen, K Caeyenberghs, I Leunissen, Linden C Vander, A Leemans, S Sunaert, J Duysens, and SP Swinnen. Training-induced improvements in postural control are accompanied by alterations in cerebellar white matter in brain injured patients. *Neuroimage Clin*, 7:240–51, 2015a.

David Drijkoningen, Karen Caeyenberghs, Inge Leunissen, Catharine Vander Linden, Stefan Sunaert, Jacques Duysens, and Stephan P. Swinnen. Training-induced improvements in postural control are accompanied by alterations in cerebellar white matter in brain injured patients. *NeuroImage: Clinical*, 7:240–251, 2015b. ISSN 22131582. doi: 10.1016/j.nicl.2014.12.006. URL http://dx.doi.org/10.1016/j.nicl.2014.12.006.

Amy E. Edwards, Onur Guven, Michael D. Furman, Qadeer Arshad, and Adolfo M. Bronstein. Electroencephalographic Correlates of Continuous Postural Tasks of Increasing Difficulty. *Neuroscience*, 395:35–48, 2018. ISSN 18737544. doi: 10.1016/j.neuroscience.2018.10.040. URL https://doi.org/10.1016/j.neuroscience.2018.10.040.

Daniel B. Ennis and Gordon Kindlmann. Orthogonal tensor invariants and the analysis of diffusion tensor magnetic resonance images. *Magnetic Resonance in Medicine*, 55(1):136–146, 2005. doi: 10.1002/mrm.20741. URL https://doi.org/10.1002%2Fmrm.20741.

Fabrizio De Vico Fallani, Laura Astolfi, Febo Cincotti, Donatella Mattia, Daria la Rocca, Elira Maksuti, Serenella Salinari, Fabio Babiloni, Balazs Vegso, Gyorgy Kozmann, and Zoltan Nagy. Evaluation of the Brain Network Organization From EEG Signals: A Preliminary Evidence in Stroke Patient. *The Anatomical Record: Advances in Integrative Anatomy and Evolutionary Biology*, 292(12):2023–2031, dec 2009. doi: 10.1002/ar.20965. URL https://doi.org/10.1002%2Far.20965.

Fabrizio De Vico Fallani, Jonas Richiardi, Mario Chavez, and Sophie Achard. Graph analysis of functional brain networks: practical issues in translational neuroscience. *Philosophical Transactions of the Royal Society B: Biological Sciences*, 369(1653):20130521, oct 2014. doi: 10.1098/rstb.2013.0521. URL https://doi.org/10.1098%2Frstb.2013.0521.

M Fuchs, M Fuchs, R Drenckhahn, R Drenckhahn, H a Wischmann, H a Wischmann, M Wagner, and M Wagner. An improved boundary element method for realistic volume- conductor modeling. *IEEE Transactions on Biomedical Engineering*, 45(8):980–997, 1998.

R. Goel, Sho Nakagome, Nishant Rao, William H. Paloski, Jose L. Contreras-Vidal, and Pranav J. Parikh. Fronto-Parietal Brain Areas Contribute to the Online Control of Posture during a Continuous Balance

Task. *Neuroscience*, 413:135–153, 2019. ISSN 18737544. doi: 10.1016/j.neuroscience.2019.05.063. URL https://doi.org/10.1016/j.neuroscience.2019.05.063.

Nina Goossens, Lotte Janssens, Karen Caeyenberghs, Geneviève Albouy, and Simon Brumagne. Differences in brain processing of proprioception related to postural control in patients with recurrent non-specific low back pain and healthy controls. *NeuroImage: Clinical*, 23(May):101881, 2019. ISSN 22131582. doi: 10.1016/j.nicl.2019.101881. URL https://doi.org/10.1016/j.nicl.2019.101881.

Alexandre Gramfort, Théodore Papadopoulo, Emmanuel Olivi, and Maureen Clerc. OpenMEEG: opensource software for quasistatic bioelectromagnetics. *Biomedical engineering online*, 9:45, 2010. ISSN 1475-925X. doi: 10.1186/1475-925X-9-45.

Caterina Gratton, Emi M. Nomura, Fernando Pérez, and Mark D'Esposito. Focal brain lesions to critical locations cause widespread disruption of the modular organization of the brain. *Journal of Cognitive Neuroscience*, 2012. ISSN 0898929X. doi: 10.1162/jocn_a_00222.

Alessandra Griffa, Philipp S. Baumann, Jean Philippe Thiran, and Patric Hagmann. Structural connectomics in brain diseases. *NeuroImage*, 80:515–526, 2013. ISSN 10538119. doi: 10.1016/j.neuroimage.2013.04.056. URL http://dx.doi.org/10.1016/j.neuroimage.2013.04.056.

Patric Hagmann, Leila Cammoun, Xavier Gigandet, Reto Meuli, Christopher J. Honey, J. Van Wedeen, and Olaf Sporns. Mapping the structural core of human cerebral cortex. *PLoS Biology*, 6(7):1479–1493, 2008. ISSN 15449173. doi: 10.1371/journal.pbio.0060159.

Timothy E. Ham and David J. Sharp. How can investigation of network function inform rehabilitation after traumatic brain injury? *Current Opinion in Neurology*, 25(6):662–669, 2012. ISSN 13507540. doi: 10.1097/WCO.0b013e328359488f.

E Hashim, E Caverzasi, N Papinutto, CE Lewis, R Jing, O Charles, S Zhang, A Lin, SJ Graham, TA Schweizer, A Bharatha, and MD Cusimano. Investigating Microstructural Abnormalities and Neurocognition in Sub-Acute and Chronic Traumatic Brain Injury Patients with Normal-Appearing White Matter: A Preliminary Diffusion Tensor Imaging Study. *Front Neurol*, 8:97, 2017.

Luke J. Hearne, Luca Cocchi, Andrew Zalesky, and Jason B. Mattingley. Reconfiguration of brain network architectures between resting-state and complexity-dependent cognitive reasoning. *Journal of Neuroscience*, 37(35):8399–8411, 2017. ISSN 15292401. doi: 10.1523/JNEUROSCI.0485-17.2017.

Frank G. Hillary and Jordan H. Grafman. Injured Brains and Adaptive Networks: The Benefits and Costs of Hyperconnectivity. *Trends in Cognitive Sciences*, 21(5):385–401, may 2017. doi: 10.1016/j.tics.2017.03.003. URL https://doi.org/10.1016%2Fj.tics.2017.03.003.

Cheng Ya Huang, Gwo Ching Chang, Yi Ying Tsai, and Ing Shiou Hwang. An increase in postural load facilitates an anterior shift of processing resources to frontal executive function in a postural-suprapostural task. *Frontiers in Human Neuroscience*, 10(August):1–16, 2016. ISSN 16625161. doi: 10.3389/fnhum.2016.00420.

T. Hülsdünker, A. Mierau, C. Neeb, H. Kleinöder, and H.K. Strüder. Cortical processes associated with continuous balance control as revealed by EEG spectral power. *Neuroscience Letters*, 592:1–5, apr 2015. doi: 10.1016/j.neulet.2015.02.049. URL https://doi.org/10.1016%2Fj.neulet.2015.02.049.

Thorben Hülsdünker, Andreas Mierau, and Heiko K. Strüder. Higher Balance Task Demands are Associated with an Increase in Individual Alpha Peak Frequency. *Frontiers in Human Neuroscience*, 9, jan 2016. doi: 10.3389/fnhum.2015.00695. URL https://doi.org/10.3389%2Ffnhum.2015.00695.

Phoebe Imms, Adam Clemente, Mark Cook, Wendyl D'Souza, Peter H. Wilson, Derek K. Jones, and Karen Caeyenberghs. The structural connectome in traumatic brain injury: A meta-analysis of graph metrics. *Neuroscience & Biobehavioral Reviews*, 99:128–137, apr 2019. doi: 10.1016/j.neubiorev.2019.01.002. URL https://doi.org/10.1016%2Fj.neubiorev.2019.01.002.

M Inglese, S Makani, G Johnson, BA Cohen, JA Silver, O Gonen, and RI Grossman. Diffuse axonal injury in mild traumatic brain injury: a diffusion tensor imaging study. *J Neurosurg*, 103:298–303, Aug 2005.

M Kasahara, D K Menon, C H Salmond, J G Outtrim, J V Taylor Tavares, T A Carpenter, B J Sahakian, and E A Stamatakis. Altered functional connectivity in the motor network after traumatic brain injury. *Neurology*, 75(2):168–176, 2010.

Kenton R. Kaufman, Robert H. Brey, Li-Shan Chou, Ann Rabatin, Allen W. Brown, and Jeffrey R. Basford. Comparison of subjective and objective measurements of balance disorders following traumatic brain injury. *Medical Engineering & Physics*, 28(3):234–239, apr 2006. doi: 10.1016/j.medengphy.2005.05.005. URL https://doi.org/10.1016%2Fj.medengphy.2005.05.005.

Wolfgang Klimesch, Robert Fellinger, and Roman Freunberger. Alpha Oscillations and Early Stages of Visual Encoding. *Frontiers in Psychology*, 2, 2011. doi: 10.3389/fpsyg.2011.00118. URL https://doi.org/10.3389%2Ffpsyg.2011.00118.

Louis-David Lord, Angus B Stevner, Gustavo Deco, and Morten L Kringelbach. Understanding principles of integration and segregation using whole-brain computational connectomics: implications for neuropsychiatric disorders. *Philosophical Transactions of the Royal Society A: Mathematical, Physical and Engineering Sciences*, 375(2096):20160283, 2017.

Scott Makeig, Anthony J Bell, Tzyy-Ping Jung, and Terrence J Sejnowski. Independent component analysis of electroencephalographic data. In *Advances in neural information processing systems*, pages 145–151, 1996.

S Marek and NUF Dosenbach. The frontoparietal network: function, electrophysiology, and importance of individual precision mapping. *Dialogues Clin Neurosci*, 20:133–140, Jun 2018.

John D. Medaglia. Functional Neuroimaging in Traumatic Brain Injury: From Nodes to Networks. *Frontiers in Neurology*, 8, aug 2017. doi: 10.3389/fneur.2017.00407. URL https://doi.org/10.3389%2Ffneur.2017.00407.

Christoph M. Michel and Denis Brunet. EEG source imaging: A practical review of the analysis steps. *Frontiers in Neurology*, 10(APR), 2019. ISSN 16642295. doi: 10.3389/fneur.2019.00325.

Andreas Mierau, Britta Pester, Thorben Hülsdünker, Karin Schiecke, Heiko K. Strüder, and Herbert Witte. Cortical Correlates of Human Balance Control. *Brain Topography*, 30(4):434–446, may 2017. doi: 10.1007/s10548-017-0567-x. URL https://doi.org/10.1007%2Fs10548-017-0567-x.

Masahito Mihara, Ichiro Miyai, Megumi Hatakenaka, Kisou Kubota, and Saburo Sakoda. Role of the prefrontal cortex in human balance control. *NeuroImage*, 43(2):329–336, 2008. ISSN 10538119. doi: 10.1016/j.neuroimage.2008.07.029.

Francesca Miraglia, Fabrizio Vecchio, and Paolo Maria Rossini. Brain electroencephalographic segregation as a biomarker of learning. *Neural Networks*, 106:168–174, oct 2018. doi: 10.1016/j.neunet.2018.07.005. URL https://doi.org/10.1016%2Fj.neunet.2018.07.005.

Tim Mullen, Christian Kothe, Mike Chi, Alejandro Ojeda, Trevor Kerth, Scott Makeig, Tzyy-Ping Jung, and Gert Cauwenberghs. Real-time Neuroimaging and Cognitive Monitoring Using Wearable Dry EEG. *IEEE Transactions on Biomedical Engineering*, 62(11):2553–2567, 2015. ISSN 0018-9294. doi: 10.1109/TBME.2015.2481482. URL http://ieeexplore.ieee.org/lpdocs/epic03/wrapper.htm?arnumber=7274673.

Tamanna T.K. Munia, Ali Haider, Charles Schneider, Mark Romanick, and Reza Fazel-Rezai. A Novel EEG Based Spectral Analysis of Persistent Brain Function Alteration in Athletes with Concussion History. *Scientific Reports*, 7(1):1–13, 2017. ISSN 20452322. doi: 10.1038/s41598-017-17414-x. URL http://dx.doi.org/10.1038/s41598-017-17414-x.

Toru Nakamura, Frank G. Hillary, and Bharat B. Biswal. Resting network plasticity following brain injury. *PLoS ONE*, 4(12), 2009. ISSN 19326203. doi: 10.1371/journal.pone.0008220.

V Newcombe, D Chatfield, J Outtrim, S Vowler, A Manktelow, J Cross, D Scoffings, M Coleman, P Hutchinson, J Coles, TA Carpenter, J Pickard, G Williams, and D Menon. Mapping traumatic axonal injury using diffusion tensor imaging: correlations with functional outcome. *PLoS One*, 6:e19214, May 2011.

M. E. J. Newman. Modularity and community structure in networks. *PNAS*, 99(12):7821–7826, jun 2006. ISSN 0027-8424. doi: 10.1073/pnas.122653799. URL https://www.pnas.org/content/103/23/8577.

SN Niogi, P Mukherjee, J Ghajar, CE Johnson, R Kolster, H Lee, M Suh, RD Zimmerman, GT Manley, and BD McCandliss. Structural dissociation of attentional control and memory in adults with and without mild traumatic brain injury. *Brain*, 131:3209–21, Dec 2008.

Guido Nolte, Ou Bai, Lewis Wheaton, Zoltan Mari, Sherry Vorbach, and Mark Hallett. Identifying true brain interaction from EEG data using the imaginary part of coherency. *Clinical Neurophysiology*, 115 (10):2292–2307, 2004. ISSN 13882457. doi: 10.1016/j.clinph.2004.04.029.

Wolfgang Omlor, Luis Patino, Ignacio Mendez-Balbuena, Jürgen Schulte-Mönting, and Rumyana Kristeva. Corticospinal beta-range coherence is highly dependent on the pre-stationary motor state. *Journal of Neuroscience*, 31(22):8037–8045, 2011.

Robert Oostenveld and Thom F Oostendorp. Validating the boundary element method for forward and inverse EEG computations in the presence of a hole in the skull. *Human brain mapping*, 17(3):179–192, 2002.

Kristine H. O'Phelan, Chad K. Otoshi, Thomas Ernst, and Linda Chang. Common Patterns of Regional Brain Injury Detectable by Diffusion Tensor Imaging in Otherwise Normal-Appearing White Matter in Patients with Early Moderate to Severe Traumatic Brain Injury. *Journal of Neurotrauma*, 35(5):739–749, mar 2018. doi: 10.1089/neu.2016.4944. URL https://doi.org/10.1089%2Fneu.2016.4944.

Christian O'Reilly, John D. Lewis, and Mayada Elsabbagh. Is functional brain connectivity atypical in autism? A systematic review of EEG and MEG studies. *PLOS ONE*, 12(5):e0175870, may 2017. doi: 10.1371/journal.pone.0175870. URL https://doi.org/10.1371%2Fjournal.pone.0175870.

JA Owens, G Spitz, JL Ponsford, AR Dymowski, and C Willmott. An investigation of white matter integrity and attention deficits following traumatic brain injury. *Brain Inj*, 32:776–783, 2018.

Anand S. Pandit, Paul Expert, Renaud Lambiotte, Valerie Bonnelle, Robert Leech, Federico E. Turkheimer, and David J. Sharp. Traumatic brain injury impairs small-world topology. *Neurology*, 80(20):1826–1833, 2013. ISSN 00283878. doi: 10.1212/WNL.0b013e3182929f38.

R D Pascual-Marqui. Standardized low-resolution brain electromagnetic tomography (sLORETA): technical details. *Methods and findings in experimental and clinical pharmacology*, 24 Suppl D:5–12, 2002. ISSN 0379-0355. URL http://www.ncbi.nlm.nih.gov/pubmed/12575463.

TC Pickett, LS Radfar-Baublitz, SD McDonald, WC Walker, and DX Cifu. Objectively assessing balance deficits after TBI: Role of computerized posturography. *J Rehabil Res Dev*, 44:983–90, 2007.

Luca Pion-Tonachini, Ken Kreutz-Delgado, and Scott Makeig. ICLabel: An automated electroencephalographic independent component classifier, dataset, and website. *NeuroImage*, 198:181–197, sep 2019. ISSN 1053-8119. doi: 10.1016/J.NEUROIMAGE.2019.05.026. URL https://www.sciencedirect.com/science/article/abs/pii/S1053811919304185.

Adam B. Rosen, Jennifer M. Yentes, Melanie L. McGrath, Arthur C. Maerlender, Sara A. Myers, and Mukul Mukherjee. Alterations in cortical activation among individuals with chronic ankle instability during single-limb postural control. *Journal of Athletic Training*, 54(6):718–726, 2019. ISSN 1938162X. doi: 10.4085/1062-6050-448-17.

Mikail Rubinov and Olaf Sporns. Complex network measures of brain connectivity: Uses and interpretations. *NeuroImage*, 52(3):1059–1069, 2010. ISSN 10538119. doi: 10.1016/j.neuroimage.2009.10.003. URL http://dx.doi.org/10.1016/j.neuroimage.2009.10.003.

J.D. Rudie, J.A. Brown, D. Beck-Pancer, L.M. Hernandez, E.L. Dennis, P.M. Thompson, S.Y. Bookheimer, and M. Dapretto. Altered functional and structural brain network organization in autism. *NeuroImage: Clinical*, 2:79–94, 2013. doi: 10.1016/j.nicl.2012.11.006. URL https://doi.org/10.1016%2Fj.nicl.2012.11.006.

D Rueckert, LI Sonoda, C Hayes, DL Hill, MO Leach, and DJ Hawkes. Nonrigid registration using free-form deformations: application to breast MR images. *IEEE Trans Med Imaging*, 18:712–21, Aug 1999.

Katiuscia Sacco, Franco Cauda, Federico D'Agata, Sergio Duca, Marina Zettin, Roberta Virgilio, Alberto Nascimbeni, Guido Belforte, Gabriella Eula, Laura Gastaldi, et al. A combined robotic and cognitive training for locomotor rehabilitation: evidences of cerebral functional reorganization in two chronic traumatic brain injured patients. *Frontiers in Human Neuroscience*, 5:146, 2011.

G. Di Scala, M. Dupuy, E. Guillaud, E. Doat, E. Barse, B. Dillhareguy, F.A.M. Jean, M. Audiffren, J.R. Cazalets, and S. Chanraud. Efficiency of Sensorimotor Networks: Posture and Gait in Young and Older Adults. *Experimental Aging Research*, 45(1):41–56, jan 2019. doi: 10.1080/0361073x.2018.1560108. URL https://doi.org/10.1080%2F0361073x.2018.1560108.

Björn Schelter, Matthias Winterhalder, Michael Eichler, Martin Peifer, Bernhard Hellwig, Brigitte Guschlbauer, Carl Hermann Lücking, Rainer Dahlhaus, and Jens Timmer. Testing for directed influences among neural signals using partial directed coherence. *Journal of neuroscience methods*, 152(1-2): 210–219, 2006.

David J. Sharp, Gregory Scott, and Robert Leech. Network dysfunction after traumatic brain injury. *Nature Reviews Neurology*, 10(3):156–166, 2014. ISSN 17594766. doi: 10.1038/nrneurol.2014.15. URL http://dx.doi.org/10.1038/nrneurol.2014.15.

Vikram Shenoy Handiru, A.P. Vinod, and Cuntai Guan. EEG Source Imaging of Movement Decoding: The State of the Art and Future Directions. *IEEE Systems, Man, and Cybernetics Magazine*, 4(2):14–23, 2018. ISSN 2380-1298. doi: 10.1109/msmc.2017.2778458.

ME Shenton, HM Hamoda, JS Schneiderman, S Bouix, O Pasternak, Y Rathi, MA Vu, MP Purohit, K Helmer, I Koerte, AP Lin, CF Westin, R Kikinis, M Kubicki, RA Stern, and R Zafonte. A review of magnetic resonance imaging and diffusion tensor imaging findings in mild traumatic brain injury. *Brain Imaging Behav*, 6:137–92, Jun 2012.

Semyon Slobounov, Tao Wu, and Mark Hallett. Neural basis subserving the detection of postural instability: An fMRI study. *Motor Control*, 2006. ISSN 15432696. doi: 10.1123/mcj.10.1.69.

Semyon Slobounov, Wayne Sebastianelli, and Mark Hallett. Residual brain dysfunction observed one year post-mild traumatic brain injury: Combined EEG and balance study. *Clinical Neurophysiology*, 123(9): 1755–1761, 2012. ISSN 13882457. doi: 10.1016/j.clinph.2011.12.022. URL http://dx.doi.org/10.1016/j.clinph.2011.12.022.

Semyon M. Slobounov, Elizabeth Teel, and Karl M. Newell. Modulation of cortical activity in response to visually induced postural perturbation: combined VR and EEG study. *Neuroscience letters*, 547:6–9, 2013. ISSN 18727972. doi: 10.1016/j.neulet.2013.05.001. URL http://dx.doi.org/10.1016/j.neulet.2013.05.001.

LGF Smith, E Milliron, ML Ho, HH Hu, J Rusin, J Leonard, and EA Sribnick. Advanced neuroimaging in traumatic brain injury: an overview. *Neurosurg Focus*, 47:E17, Dec 2019.

SM Smith, M Jenkinson, MW Woolrich, CF Beckmann, TE Behrens, H Johansen-Berg, PR Bannister, Luca M De, I Drobnjak, DE Flitney, RK Niazy, J Saunders, J Vickers, Y Zhang, Stefano N De, JM Brady,

and PM Matthews. Advances in functional and structural MR image analysis and implementation as FSL. *Neuroimage*, 23 Suppl 1:S208–19, 2004.

SM Smith, M Jenkinson, H Johansen-Berg, D Rueckert, TE Nichols, CE Mackay, KE Watkins, O Ciccarelli, MZ Cader, PM Matthews, and TE Behrens. Tract-based spatial statistics: voxelwise analysis of multi-subject diffusion data. *Neuroimage*, 31:1487–505, Jul 2006.

SM Smith, H Johansen-Berg, M Jenkinson, D Rueckert, TE Nichols, KL Miller, MD Robson, DK Jones, JC Klein, AJ Bartsch, and TE Behrens. Acquisition and voxelwise analysis of multi-subject diffusion data with tract-based spatial statistics. *Nat Protoc*, 2:499–503, 2007.

Teodoro Solis-Escalante, Joris van der Cruijsen, Digna de Kam, Joost van Kordelaar, Vivian Weerdesteyn, and Alfred C. Schouten. Cortical dynamics during preparation and execution of reactive balance responses with distinct postural demands. *NeuroImage*, 188(September 2018):557–571, 2019. ISSN 10959572. doi: 10.1016/j.neuroimage.2018.12.045. URL https://doi.org/10.1016/j.neuroimage.2018.12.045.

G Spitz, JJ Maller, R O'Sullivan, and JL Ponsford. White matter integrity following traumatic brain injury: the association with severity of injury and cognitive functioning. *Brain Topogr*, 26:648–60, Oct 2013.

Olaf Sporns. Network attributes for segregation and integration in the human brain. *Current opinion in neurobiology*, 23(2):162–171, 2013.

Cornelis J. Stam. Modern network science of neurological disorders. *Nature Reviews Neuroscience*, 15(10): 683–695, 2014. ISSN 1471-003X. doi: 10.1038/nrn3801. URL http://dx.doi.org/10.1038/nrn3801.

OJ Surgent, OI Dadalko, KA Pickett, and BG Travers. Balance and the brain: A review of structural brain correlates of postural balance and balance training in humans. *Gait Posture*, 71:245–252, Jun 2019.

Franois Tadel, Sylvain Baillet, John C. Mosher, Dimitrios Pantazis, and Richard M. Leahy. Brainstorm: A user-friendly application for MEG/EEG analysis. *Computational Intelligence and Neuroscience*, 2011, 2011. ISSN 16875265. doi: 10.1155/2011/879716.

Kaoru Takakusaki. Functional Neuroanatomy for Posture and Gait Control. *Journal of Movement Disorders*, 10(1):1–17, jan 2017. doi: 10.14802/jmd.16062. URL https://doi.org/10.14802%2Fjmd.16062.

I. V. Talalay, A. V. Kurgansky, and R. I. Machinskaya. Alpha-band functional connectivity during cued versus implicit modality-specific anticipatory attention: EEG-source coherence analysis. *Psychophysiology*, 55(12):e13269, jul 2018. doi: 10.1111/psyp.13269. URL https://doi.org/10.1111%2Fpsyp.13269.

Marco Taubert, Jan Mehnert, Burkhard Pleger, and Arno Villringer. Rapid and specific gray matter changes in M1 induced by balance training. *NeuroImage*, 133:399–407, 2016. ISSN 10959572. doi: 10.1016/j.neuroimage.2016.03.017. URL http://dx.doi.org/10.1016/j.neuroimage.2016.03.017.

Christopher A. Taylor, Jeneita M. Bell, Matthew J. Breiding, and Likang Xu. Traumatic Brain Injury–Related Emergency Department Visits, Hospitalizations, and Deaths — United States, 2007 and 2013. *MMWR. Surveillance Summaries*, 66(9):1–16, mar 2017. ISSN 1546-0738. doi: 10.15585/mmwr.ss6609a1. URL http://www.cdc.gov/mmwr/volumes/66/ss/ss6609a1.htm.

MN Uddin, TD Figley, KG Solar, AS Shatil, and CR Figley. Comparisons between multi-component myelin water fraction, T1w/T2w ratio, and diffusion tensor imaging measures in healthy human brain structures. *Sci Rep*, 9:2500, Feb 2019.

Rene L. Utianski, John N. Caviness, Elisabeth C.W. van Straaten, Thomas G. Beach, Brittany N. Dugger, Holly A. Shill, Erika D. Driver-Dunckley, Marwan N. Sabbagh, Shyamal Mehta, Charles H. Adler, and Joseph G. Hentz. Graph theory network function in Parkinson's disease assessed with electroencephalography. *Clinical Neurophysiology*, 127(5):2228–2236, may 2016. doi: 10.1016/j.clinph.2016.02.017. URL https://doi.org/10.1016%2Fj.clinph.2016.02.017.

Frederik Van de Steen, Luca Faes, Esin Karahan, Jitkomut Songsiri, Pedro A. Valdes-Sosa, and Daniele Marinazzo. Critical Comments on EEG Sensor Space Dynamical Connectivity Analysis. *Brain Topography*, 32(4):643–654, 2019. ISSN 15736792. doi: 10.1007/s10548-016-0538-7.

Jessy Parokaran Varghese, William R. Staines, and William E. McIlroy. Activity in Functional Cortical Networks Temporally Associated with Postural Instability. *Neuroscience*, 401:43–58, 2019. ISSN 18737544. doi: 10.1016/j.neuroscience.2019.01.008. URL https://doi.org/10.1016/j.neuroscience.2019.01.008.

V Veeramuthu, V Narayanan, TL Kuo, L Delano-Wood, K Chinna, MW Bondi, V Waran, D Ganesan, and N Ramli. Diffusion Tensor Imaging Parameters in Mild Traumatic Brain Injury and Its Correlation with Early Neuropsychological Impairment: A Longitudinal Study. *J Neurotrauma*, 32:1497–509, Oct 2015.

Umesh M. Venkatesan and Frank G. Hillary. Functional connectivity within lateral posterior parietal cortex in moderate to severe traumatic brain injury. *Neuropsychology*, 33(6):893–910, sep 2019. doi: 10.1037/neu0000553. URL https://doi.org/10.1037%2Fneu0000553.

Gerald T. Voelbel, Helen M. Genova, Nancy D. Chiaravalotti, and Matthew J. Hoptman. Diffusion tensor imaging of traumatic brain injury review: Implications for neurorehabilitation. *NeuroRehabilitation*, 31 (3):281–293, sep 2012. doi: 10.3233/nre-2012-0796. URL https://doi.org/10.3233%2Fnre-2012-0796.

Erica J. Wallace, Jane L. Mathias, and Lynn Ward. Diffusion tensor imaging changes following mild moderate and severe adult traumatic brain injury: a meta-analysis. *Brain Imaging and Behavior*, 12(6):1607–1621, jan 2018. doi: 10.1007/s11682-018-9823-2. URL https://doi.org/10.1007%2Fs11682-018-9823-2.

Bitan Wang, Ming Zhang, Lingguo Bu, Liwei Xu, Wei Wang, and Zengyong Li. Posture-related changes in brain functional connectivity as assessed by wavelet phase coherence of NIRS signals in elderly subjects. *Behavioural Brain Research*, 312:238–245, 2016. ISSN 18727549. doi: 10.1016/j.bbr.2016.06.037. URL http://dx.doi.org/10.1016/j.bbr.2016.06.037.

Ellen Wittenberg, Jessica Thompson, Chang S. Nam, and Jason R. Franz. Neuroimaging of human balance control: A systematic review. *Frontiers in Human Neuroscience*, 11(April):1–25, 2017. ISSN 16625161. doi: 10.3389/fnhum.2017.00170.

JR Wozniak, L Krach, E Ward, BA Mueller, R Muetzel, S Schnoebelen, A Kiragu, and KO Lim. Neurocognitive and neuroimaging correlates of pediatric traumatic brain injury: a diffusion tensor imaging (DTI) study. *Arch Clin Neuropsychol*, 22:555–68, Jun 2007.

Mingrui Xia, Jinhui Wang, and Yong He. BrainNet Viewer: A Network Visualization Tool for Human Brain Connectomics. *PLoS ONE*, 8(7):e68910, jul 2013. doi: 10.1371/journal.pone.0068910. URL https://doi.org/10.1371%2Fjournal.pone.0068910.

Yuliya N. Yoncheva, Krishna Somandepalli, Philip T. Reiss, Clare Kelly, Adriana Di Martino, Mariana Lazar, Juan Zhou, Michael P. Milham, and F. Xavier Castellanos. Mode of Anisotropy Reveals Global Diffusion Alterations in Attention-Deficit/Hyperactivity Disorder. *Journal of the American Academy of Child & Adolescent Psychiatry*, 55(2):137–145, feb 2016. doi: 10.1016/j.jaac.2015.11.011. URL https://doi.org/10.1016%2Fj.jaac.2015.11.011.

Yongxia Zhou. Small world properties changes in mild traumatic brain injury. *Journal of magnetic resonance imaging : JMRI*, 46(2):518–527, 2017. ISSN 1522-2586. doi: 10.1002/jmri.25548. URL http://www.ncbi.nlm.nih.gov/pubmed/27902865http://www.pubmedcentral.nih.gov/articlerender.fcgi?artid=PMC5449268.